

# All-path-length and sub-eikonal corrections to momentum broadening in the opacity expansion approach.

Dario van den Berg<sup>1, 2, 3, \*</sup> and Isobel Kolb  <sup>1, 2, 3, †</sup>

<sup>1</sup>*School of Physics, University of the Witwatersrand, Johannesburg 2000, South Africa*

<sup>2</sup>*Mandelstam Institute for Theoretical Physics (MITP),  
University of the Witwatersrand, Johannesburg 2000, South Africa*

<sup>3</sup>*National Institute for Theoretical and Computational Sciences (NITheCS), Stellenbosch 7600, South Africa*

(Dated: February 19, 2026)

## I. ABSTRACT

We present a detailed study of momentum broadening for high-energy partons traversing the Quark-Gluon Plasma (QGP), extending the Gyulassy-Levai-Vitev (GLV) formalism to include both all-path-length (APL) and sub-eikonal corrections. Traditional GLV calculations rely on the large separation distance and large formation time approximations, which are valid for large systems, but whose applicability in small systems such as pp and p/dA may fail. We derive analytic expressions for the momentum broadening distributions to first order in the opacity expansion, and perform a numerical investigation to quantify their impact. Our results show that the APL result reduces the low-momentum broadening and the sub-eikonal correction enhances the high-momentum broadening. The combined APL and sub eikonal correction show that the sub-eikonal correction mitigates the effect of the APL correction.

## II. INTRODUCTION

The study of quark-gluon-plasma (QGP) formation has traditionally focused on relativistic heavy-ion collisions, where large systems of deconfined matter are produced under extreme energy densities [1]. The QGP is a strongly interacting phase of QCD in which quarks and gluons become deconfined over extended volumes, forming a nearly perfect fluid with extremely low shear viscosity over entropy density  $\eta/s$  [2, 3]. Its properties are encoded in transport coefficients and response functions that can be probed by hard partons produced in the early stages of the collision.

High-energy quarks and gluons traversing the QGP are predicted to undergo multiple scatterings, leading to jet quenching, a suppression and modification of high- $p_T$  observables relative to proton-proton expectations [4, 5]. Among others, jet quenching is observed through reduced yields of high- $p_T$  hadrons and jets [6–10] and medium-induced modifications to jet substructure [11–14]. A key component of jet quenching is momentum broadening, the stochastic transverse momentum accumulation of a propagating parton due to repeated soft scatterings with medium constituents [15, 16].

Perturbative Quantum Chromodynamics (pQCD)-based energy loss models [17] such as GLV [18–23], BDMPS-Z [15, 24–26], and ASW [27] have been extremely successful in quantitatively describing the observed jet quenching patterns in nucleus-nucleus (AA) collisions at RHIC and the LHC [28, 29]. These frameworks incorporate both collisional and radiative energy loss [30] and have achieved remarkable consistency across diverse observables, such as the nuclear modification factor  $R_{AA}$  [31] and jet shape broadening [32]. Their success has made pQCD energy-loss formalisms central tools for extracting QGP transport coefficients, and for understanding the behavior of QCD matter at extreme temperatures and densities.

However, recent experimental results have revealed QGP-like signatures even in small collision systems such as high-multiplicity proton-proton (pp) and proton-lead (pPb) collisions. Observables including collective multi-particle correlations [33], strangeness enhancement [34], and quarkonium suppression [35], previously considered exclusive to large systems, have also been reported in much smaller collision systems. These findings raise fundamental questions about the minimal conditions necessary for QGP formation, the role of initial-state correlations or saturation physics,

\* [dario.vandenberg@gmail.com](mailto:dario.vandenberg@gmail.com)

† [isobel.kolbe@wits.ac.za](mailto:isobel.kolbe@wits.ac.za)

and whether a short-lived, deconfined medium can emerge in systems with limited size and lifetime [33]. For reviews of extensive results, see [17].

The first oxygen-oxygen, proton-oxygen, and neon-neon collision runs at the LHC highlight the growing need to understand energy loss, transverse momentum broadening, and medium formation in intermediate-sized systems. These collisions provide unprecedented opportunities to probe the onset of QGP-like behavior with controlled variations in system size, multiplicity, and nuclear geometry. In particular, they allow tests of whether jet quenching, collectivity, and strangeness enhancement persist as the number of participants decreases, thereby offering key constraints on initial-state modeling, small-system hydrodynamics, and the possible emergence of a short-lived, strongly interacting medium [36, 37]. The OO and NeNe datasets thus play a crucial role in determining the applicability limits of pQCD energy-loss frameworks and in distinguishing genuine medium-induced phenomena from alternative explanations such as color reconnection or gluon saturation dynamics.

Recent theoretical developments further motivate the possibility that OO and NeNe collisions may already lie within a regime where QGP-like dynamics become relevant [38–40]. The analysis in [41] further demonstrates that a single, smoothly varying medium parameter can describe nuclear modification patterns from pp and pA through OO and up to PbPb. Such continuity strongly suggests that even intermediate-sized systems may achieve densities sufficient for partial color deconfinement and multiple scattering, supporting the interpretation that QGP-like matter can form below the traditionally assumed system-size threshold.

Further support for the relevance of medium-induced interactions in these systems comes from the global analysis presented in [42, 43], which highlights the essential role of transverse momentum broadening and elastic energy loss in describing suppression patterns across all collision systems. The extracted fits require nonzero elastic contributions even in the smallest systems, indicating nontrivial momentum broadening. In particular, the suppression exhibits a maximum around  $p_T \sim 7$  GeV, a transitional region where the probe is neither fully hydrodynamic nor asymptotically hard, and where purely eikonal approximations are known to lose accuracy [41]. This behavior naturally points to sensitivity to path-length-dependent scattering and sub-eikonal corrections. These conclusions are consistent with recent theoretical studies emphasizing the importance of transverse momentum broadening, elastic scattering, and sub-eikonal corrections in small and intermediate collision systems [44]. A detailed theoretical treatment of momentum broadening and elastic scattering therefore becomes essential, as such effects may offer some of the earliest and most sensitive indicators of medium formation in these new LHC and RHIC collision systems.

Conventional jet quenching models, such as the Gyulassy–Levai–Vitev (GLV) formalism [18–23], rely on several approximations that are valid in large systems but may break down in smaller collision systems. These include:

- **Large separation distance:** In the GLV approach, the distance  $\Delta z = z_1 - z_0$  between the hard parton production point  $z_0$  and the first scattering center  $z_1$  satisfies  $\Delta z \gg \lambda_{mfp} \gg 1/\mu_D$ , where  $\lambda_{mfp}$  is the parton mean free path and  $\mu_D$  the Debye screening mass. While it is crucial that  $\lambda_{mfp} \gg 1/\mu_D$ , small colliding systems necessarily select for events in which  $\Delta z \sim 1/\mu_D$ .
- **Large formation time:** When including radiation, GLV assumes that the gluon formation time  $\tau \gg 1/\mu_D$ , where  $\tau \sim \frac{xP^+}{\mathbf{k}^2}$ , and  $\mathbf{k}$  is the transverse momentum of the radiated gluon.

While the broadening has been computed in the GLV formalism [18–23, 45, 46], even including a flowing medium [47], it is not straightforward to relax the above approximations. The first attempt to correct for the large system approximation [48, 49] revealed that, while the large formation time approximation played only a small role in the usual approximation scheme, when relaxing the large separation distance approximation, the large formation time approximation meant that the majority of diagrams did not have an all-path length contribution. That is to say that, due to the large formation time approximation, all most all path-length corrections remained suppressed. One of the major results of [48, 49] was that the all path-length correction is negative and dominates at large energies, suggesting that dampening corrections are missing.

Relaxing the large formation time approximation along with the large separation distance approximation in the full radiative energy-loss case is an enormous undertaking. As such, in this work we will relax both approximations for the simpler broadening case. One may additionally argue that, since broadening (and quenching) effects are more pronounced at lower partonic energies [50], and the effect is expected to be small in small systems due to the shorter pathlength [42, 43], one may consider partonic energies that are not infinitely higher than the momentum scale of the medium in order to detect quenching effects. However, this violates the broadening analogue of the large formation time approximation which requires  $P^+ \gg \mathbf{q}$  (see [18–23, 45, 46]), further motivating the present work in which sub-eikonal corrections are computed.

In this work we will refer to the following corrections to the standard GLV calculation:

1. *All-path-length (APL) corrections*, which relax the large separation distance approximation by accounting for contributions from all possible scattering distances.
2. *Sub-eikonal corrections*, which retain correction terms to the  $1/P^+$  expansion, analogous to capturing the finite formation time effects in the radiative case.

We will apply each of these corrections in turn, as well as simultaneously, showing clearly that, corrections to the APL result moderate the effect of the APL correction. This result suggests that the full radiative APL result may be moderated by the inclusion of a sub-eikonal correction (See fig. 4a and fig. 4b) (a task which is well beyond the scope of the present work).

In this work, we also highlight the crucial role of unitarity. Because we are calculating corrections to the momentum broadening distribution, our results must remain consistent with unitarity, as in the original GLV broadening calculation. In particular, unitarity imposes constraints on sub-eikonal corrections: simply relaxing the eikonal approximation without care can lead to unitarity violation. For a detailed discussion of unitarity preservation, see section III, and for how we computed a sub-eikonal result consistent with unitarity, see section A.

This paper is organised as follows. In section III, we introduce the GLV framework for calculating the momentum-broadening distribution, including a detailed discussion of unitarity in section III. In section IV, we review the approximations underlying the GLV formalism, discuss their physical motivation, and outline how these approximations are systematically relaxed. The main analytical results of the paper are presented in section V, with the full derivation provided in a section A. Finally, in section VI, we perform a numerical study and present several figures illustrating the impact of the corrections. We conclude with a brief discussion of several formal subtleties in section B.

### III. SETUP

We start by reproducing the GLV setup for ease of reference, before presenting modifications that allow for the calculation of the APL and sub-eikonal corrections. A high momentum parton produced at an initial position  $(t_0, z_0, \mathbf{x}_0)$  within a finite QGP medium. Throughout, we denote two-dimensional transverse (to the motion of the parton) vectors in boldface as  $\mathbf{p}$ , three-dimensional spatial vectors as  $\vec{p} = (p_z, \mathbf{p})$ , and four-vectors in Minkowski or light-cone coordinates as  $p = (p^0, \vec{p}) = [p^0 + p^z, p^0 - p^z, \mathbf{p}]$  respectively. The magnitude of  $\mathbf{p}$  and  $\mathbf{q}$  are denoted as  $p_\perp = |\mathbf{p}|$  and  $q_\perp = |\mathbf{q}|$ . The target scattering center is modelled by a Gyulassy–Wang Debye-screened potential [18] with Fourier and color structure

$$V_n = V(\mathbf{q}_n) e^{-i\mathbf{q}_n \cdot \mathbf{x}_n} = 2\pi\delta(q^0) v(q_n, q_n^z) e^{-i\mathbf{q}_n \cdot \mathbf{x}_n} T_{a_n}(R) \otimes T_{a_n}(n), \quad (1)$$

with the Yukawa-screened form

$$v(\vec{q}) = \frac{4\pi\alpha_s}{\vec{q}^2 + \mu^2}, \quad (2)$$

and  $q_{1,0} = q_{2,0} = 0$ , since the potential is static and does not vary with time. The color exchanges are handled using the appropriate  $SU(N_c)$  generators:  $T_a(n)$  in the  $d_n$ -dimensional representation of the target, or  $T_a(R)$  in the  $d_R$ -dimensional representation of the high- $p_T$  parent parton.

The relevant diagrams at leading order in the opacity are shown in fig. 1. The initial transverse-momentum profile of jets produced by the hard scattering is highly collimated :

$$\frac{dN^{(0)}}{d^3\vec{p}} = \frac{1}{2(2\pi)^3} |J(p)|^2 = f(E) \delta^{(2)}(\mathbf{p}). \quad (3)$$

Here  $f(E)$  encodes the momentum dependence of the parton, where  $E$  is the parton's initial energy. In the traditional GLV framework, one finds  $f(E) = 1/E^4$ . In section B, we derive this form in detail and discuss several formal subtleties associated with this result.

The full jet distribution, to first order in opacity, is given by (as in [45])

$$\frac{dN^{(1)}}{d^3\vec{p}} = \int \rho(\Delta z) \int d^2\mathbf{q} \bar{\sigma}(\mathbf{q}) \left[ \frac{dN^{(0)}}{d^2(\mathbf{p} - \mathbf{q})dP^+} - \frac{dN^{(0)}}{d^2\mathbf{p} dP^+} \right], \quad (4)$$

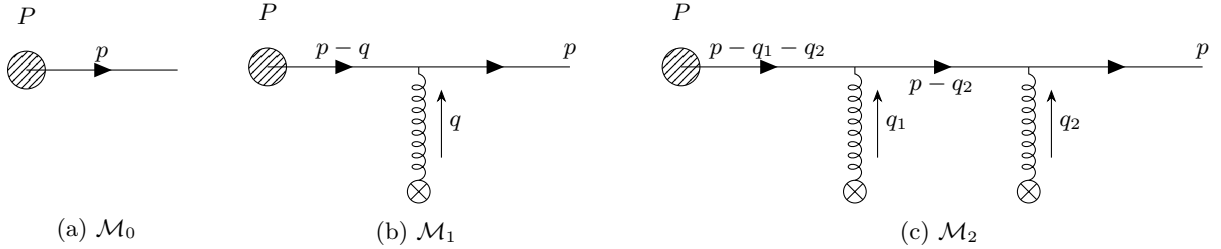


FIG. 1: The relevant Feynman diagrams for momentum broadening at leading order in the opacity.

where the first order opacity in terms of matrix elements is given by

$$\frac{dN^{(1)}}{d^3\vec{p}} = \left( \frac{1}{d_T} \text{Tr} \langle |\mathcal{M}_1|^2 \rangle + \frac{2}{d_T} \text{Re} \text{Tr} \langle \mathcal{M}_2 \mathcal{M}_0^* \rangle \right), \quad (5)$$

and the color traces and average over impact parameter give

$$\text{Tr} \langle T_a(j) T_a(R) T_a^*(j) T_a^*(R) \rangle = C^2(R) d_R = \frac{d_R}{d_A} C_2(R) C(R), \quad (6)$$

$$\langle e^{-i(\mathbf{q}_1 + \mathbf{q}_2) \cdot \mathbf{b}} \rangle = \frac{(2\pi)^2}{A_\perp} \delta^{(2)}(\mathbf{q}_1 + \mathbf{q}_2), \quad (7)$$

In the contact limit, the longitudinal separation between scatterings in the double scattering diagrams satisfies  $z_2 - z_0 \rightarrow z_1 - z_0 \equiv \Delta z$ . When performing the  $\mathbf{q}_2$  integration, the delta function enforces  $\mathbf{q}_1 = -\mathbf{q}_2$ . Consequently,

$$\sum_{j=1}^N e^{-i(\mathbf{q}_1 + \mathbf{q}_2) \Delta z} = \sum_{j=1}^N e^0 = \sum_{j=1}^N 1 = N, \quad (8)$$

and the source function reduces as

$$J(p - \mathbf{q}_1 - \mathbf{q}_2) = J(p - \mathbf{q}_1 + \mathbf{q}_1) = J(p). \quad (9)$$

Lastly, one is free to choose the distribution of scattering centres. An exploration of the effect of the choice of distribution is beyond the scope of the present work, but see [48] for a discussion on different choices. We will employ the exponential distribution as in GLV:

$$\int \rho(\Delta z) = \frac{2}{L} \int_0^\infty (d\Delta z) e^{-\frac{2\Delta z}{L}}. \quad (10)$$

### Unitarity

A crucial aspect of the present analysis is unitarity. In the context of momentum broadening, preserving unitarity amounts to ensuring that the particle number remains conserved. Any correction to the broadening distribution must, therefore, satisfy  $\int d^3\vec{p} dN^{(1)}/d^3\vec{p} = 0$ . Following Refs. [45, 47], we define

$$\bar{\sigma}(\mathbf{q}) \equiv \frac{d\sigma}{d^2\mathbf{q}} = |v(\mathbf{q})|^2, \quad (11)$$

where  $\sigma_0 = \int d^2\mathbf{q} \bar{\sigma}(\mathbf{q})$ . With this definition, one may rewrite eq. (5) as

$$\frac{dN^{(1)}}{d^3\vec{p}} = \frac{N}{A_\perp} \frac{1}{d_A} C_2(R) C(R) \int \rho(\Delta z) \int \frac{d^2\mathbf{q}}{(2\pi)^2} (|J(p - \mathbf{q})|^2 - |J(p)|^2) \bar{\sigma}(\mathbf{q}) \quad (12)$$

$$= \frac{N}{A_\perp} \frac{1}{d_A} C_2(R) C(R) \int \rho(\Delta z) \int \frac{d^2\mathbf{q}}{(2\pi)^2} |J(p - \mathbf{q})|^2 (\bar{\sigma}(\mathbf{q}) - \sigma_0 \delta^{(2)}(\mathbf{q})) \quad (13)$$

$$\approx \frac{N}{A_\perp} \frac{1}{d_A} C_2(R) C(R) |J(p)|^2 \int \rho(\Delta z) \int \frac{d^2\mathbf{q}}{(2\pi)^2} (\bar{\sigma}(\mathbf{q}) - \sigma_0 \delta^{(2)}(\mathbf{q})). \quad (14)$$

The contributions from the single- and double-scattering diagrams are therefore incorporated through an effective shift in the elastic cross section,  $\bar{\sigma}(\mathbf{q}) \rightarrow \bar{\sigma}(\mathbf{q}) - \sigma_0 \delta^{(2)}(\mathbf{q})$ . As a result, the jet broadening process is unitary, since  $\int d^3 \vec{p} \frac{dN}{d^3 \vec{p}} = 0$ , which implies that the total number of final state particles is conserved and that the effect of first-order scattering is solely to redistribute transverse momentum, leading to broadening rather than particle production or loss. In order for this unitary structure to be guaranteed, the broadening distribution must factorise as

$$\frac{dN^{(1)}}{d^3 \vec{p}} = \frac{N}{A_\perp} \frac{1}{d_A} C_2(R) C(R) \int \rho(\Delta z) \int \frac{d^2 \mathbf{q}}{(2\pi)^2} (|J(p - \mathbf{q})|^2 - |J(p)|^2) f(\mathbf{q}). \quad (15)$$

Where  $f(\mathbf{q})$  is the resultant function of the propagator and potential after the  $\int dq_z$  has been performed. One may then perform a shift in integration variables,  $\mathbf{p} \rightarrow \mathbf{q} + \mathbf{p}$ . Under this transformation, the single-scattering amplitude shifts as  $J(\mathbf{p} - \mathbf{q}) \rightarrow J(\mathbf{p})$ , leading to an exact cancellation between the single- and double-scattering contributions. Consequently,  $\int d^3 \vec{p} \frac{dN^{(1)}}{d^3 \vec{p}} = 0$ , ensuring the preservation of unitarity. To guarantee this factorised form, it is essential that the function  $f(\mathbf{q})$  appearing in  $\text{Tr}\langle|\mathcal{M}_1|^2\rangle$  be identical to that arising from  $\text{Tr}\langle\mathcal{M}_2\mathcal{M}_0^*\rangle$ . The sum of the single- and double-scattering contributions must therefore take the form

$$J(\mathbf{p} - \mathbf{q})f(\mathbf{q}) - J(\mathbf{p})f(\mathbf{q}) = (J(\mathbf{p} - \mathbf{q}) - J(\mathbf{p}))f(\mathbf{q}). \quad (16)$$

We have belaboured this well-known statement about unitarity because it is crucial in the computation of the next-to-leading order contributions to the eikonal expansion performed in the present work. On the one hand unitarity provides conditions under which the expressions for the amplitudes involved are dramatically simplified. On the other hand, unitarity ensures that the cross-diagram does not contribute to the double-scattering amplitude, as described in section B

#### IV. APPROXIMATIONS

The GLV formalism relies on a set of well-defined simplifying approximations that accurately describe parton energy loss in large collision systems such as nucleus–nucleus (AA) collisions. However, the validity of these approximations becomes less certain in the context of small collision systems. Consequently, examining the impact of systematically relaxing these approximations provides the central motivation for the present study.

We will focus on two approximations in particular: the large separation distance and the large formation time approximations. The former was first relaxed in [48, 49] where the impact of the second was realised. The impact of the second can also be seen in [47] and, as such, the present work presents a step towards reducing the second.

*Large separation distance approximation* : This approximation accounts for the spatial separation between the production point  $z_0$  and the first scattering point  $z_1$ . In principle, this approximation enforces the notion that the mean free path should be larger than the screening length of the scattering centre, an assumption that is crucial for the validity of the Gyulassy-Wang model:

$$(z_1 - z_0) \gg \lambda_{mfp} \implies \mu_D \Delta z \gg 1. \quad (17)$$

In practice then, all terms proportional to  $e^{-\mu_D \Delta z}$  are neglected under the large separation distance approximation. However, the statement that  $\mu_D \Delta z \gg 1$  enforces  $\lambda_{mfp} \gg 1/\mu_D$  is not exactly correct, so that it must be possible to include contributions with small initial separation distances. The first attempt at computing an all-system-size correction to GLV energy-loss [48, 49] relaxed precisely this approximation in the full radiative energy-loss calculation, keeping terms proportional to  $e^{-\mu_D \Delta z}$ . In the present work, we will also relax this approximation, calling the result the “all-path-length” (APL) result.

*Eikonal approximation*: In the high-energy limit, the initial energy of the parent parton is taken as the largest scale, which leads to a separation of scales in the radiative case:  $2E = P^+ \gg \mathbf{k}$ . The high-energy (or, eikonal) limit leads to a hierarchy of scales:

$$\mathbf{k} \ll P^+ \implies \omega_0 = \frac{\mathbf{k}^2}{P^+} \ll \mathbf{k} \ll P^+, \quad (18)$$

In the case of radiative energy-loss, the eikonal approximation manifests as a “large formation time” approximation in which the formation time of the radiated gluon is taken to be much larger than the Debye screening length. The formation time  $\tau$  is given by

$$\frac{1}{\tau} = \frac{\mathbf{k}^2}{xP^+} \ll \mu_D \quad (19)$$

In the present analysis, which focuses on the momentum broadening case (neglecting gluon radiation), the concept of a large formation time naturally does not apply, as  $\mathbf{k} = 0$ . Nevertheless, similar terms appear in the broadening calculation. Since  $\mathbf{k} \sim \mathbf{q}$ , an appropriate broadening analogue of the “large formation time” approximation would be

$$\frac{1}{\tau_B} = \frac{\mathbf{q}^2}{P^+} \ll \mu, \quad (20)$$

where  $\mu^2 = \mu_D^2 + \mathbf{q}^2$ . The condition in eq. (20), states that the time scale associated with transverse momentum kicks in the medium is parametrically larger than the microscopic interaction scale characterized by  $\mu$ . Under this assumption, one recovers the standard eikonal separation of scales,

$$\frac{\mathbf{q}^2}{P^+} \ll \mathbf{q} \sim \mu \ll P^+ \quad (21)$$

The major contribution of the present work is to compute the next-to-leading order corrections to the eikonal approximation. In particular, in this work, we show that the calculation remains under perturbative control in the extended kinematic range

$$\mu_D \leq \mathbf{q} \leq \frac{\sqrt{2}}{2} P^+ \quad (22)$$

thus significantly enlarging the domain of applicability compared to the conventional eikonal treatment.

There are some formal subtleties associated with the sub-eikonal correction, especially at higher orders. One is the question of the cross-diagram in the double scattering amplitude. In section B we demonstrate that this diagram will not contribute provided unitarity is preserved. The other is to what extent the source term  $J(\mathbf{p})$  varies slowly with  $\mathbf{p}$ . We demonstrate in section B that the source term varies slowly with  $\mathbf{p}$  up to order  $1/(P^+)^4$ .

## V. CALCULATION

To fully investigate the effects of relaxing the *large separation distance* and *eikonal* approximations we revert back to where approximations were first used; the kinematics. In the case of the APL correction we use the original GLV kinematics as the large separation distance approximation is only applied when computing the matrix elements. In the case of the sub-eikonal correction we keep a  $q_z$  factor that is neglected in the eikonal approximation in the GLV case. The kinematics are summarized in table I.

When computing the matrix elements, the modification of the kinematics in the sub-eikonal correction introduces corrections to the poles in the propagator. The poles of the propagator now take the form  $q_z^\pm = -\frac{\sqrt{2}}{2} P^+ (1 \pm \gamma) \pm i\epsilon$ , where we introduce the “all order factor”  $\gamma \equiv \sqrt{1 - \frac{2\mathbf{q}^2}{P^{+2}}}$ . In the standard GLV calculation, the eikonal approximation is applied and only the leading term in the Taylor expansion of  $\gamma$  is used. We call  $\gamma$  the “all order factor” since it, in principle, corrects the poles to all orders in  $P^+$ . Despite  $\gamma$  capturing the behaviour to all orders in  $P^+$ , our calculation is only valid up to  $\mathcal{O}(1/P^{+3})$  as the amplitude for  $2 \rightarrow 2$  scattering in the s-channel takes the form  $J(p) \sim 1/P^{+4}$ . Computing the full source amplitude (see section B for details), one finds  $J(p) \sim 1/(P^+ + \mathbf{q})^4$ . Thus there are sub-eikonal corrections to the amplitude that would play a part in  $\mathcal{O}(1/P^{+4})$ . Furthermore there is also the case of the crossed diagram, which takes the same form as (fig. 1c) but with a crossing of the incoming gluons. This diagram produces the same result as (fig. 1c) in the contact limit but has a  $\mathcal{O}(1/P^{+4})$  correction in the well separated case.

Using the set of kinematics for the sub-eikonal case, we proceed to compute the single scattering-diagram’s matrix element  $\mathcal{M}_1$  (fig. 1b). We perform the integral  $\int dq_z$  with the updated kinematics in the sub-eikonal case. Thereafter we compute the double scattering-diagram  $\mathcal{M}_2$  (fig. 1c), which is then multiplied with the non interacting diagram

Correction Scheme	Kinematics
GLV	$P = [P^+, 0^-, \mathbf{0}] = \left( \frac{1}{\sqrt{2}} P^+, \frac{1}{\sqrt{2}} P^+, \mathbf{0} \right),$ $q = \left[ \frac{1}{\sqrt{2}} q_z, -\frac{1}{\sqrt{2}} q_z, \mathbf{q} \right] = (0_0, q_z, \mathbf{q}),$ $p = \left[ P^+ + \frac{1}{\sqrt{2}} q_z, -\frac{1}{\sqrt{2}} q_z, \mathbf{q} \right] = (p_0, p_z, \mathbf{q})$
GLV+APL	Same as GLV
(GLV) <sub>SUB</sub>	$P = [P^+, 0^-, \mathbf{0}] = \left( \frac{1}{\sqrt{2}} P^+, \frac{1}{\sqrt{2}} P^+, \mathbf{0} \right),$ $q = \left[ \frac{1}{\sqrt{2}} q_z, -\frac{1}{\sqrt{2}} q_z, \mathbf{q} \right] = (0_0, q_z, \mathbf{q}),$ $p = \left[ P^+ + \frac{1}{\sqrt{2}} q_z, -\frac{1}{\sqrt{2}} q_z, \mathbf{q} \right] = (p_0, p_z, \mathbf{q})$
(GLV+APL) <sub>SUB</sub>	Same as (GLV) <sub>SUB</sub>

TABLE I: Kinematics for different approximation schemes to momentum broadening considered in the present work.

Correction Scheme	$dN^{(1)}/d^3\vec{p}$
GLV	$\frac{N}{A_\perp} \frac{1}{d_A} C_2(R) C(R) (4\pi\alpha_s)^2 \int \rho(\Delta z) \int \frac{d^2\mathbf{q}}{(2\pi)^2} \left(  J(p - \mathbf{q}) ^2 -  J(p) ^2 \right) \frac{1}{2\mu^4}$
GLV+APL	$\frac{N}{A_\perp} \frac{1}{d_A} C_2(R) C(R) (4\pi\alpha_s)^2 \int \rho(\Delta z) \int \frac{d^2\mathbf{q}}{(2\pi)^2} \left(  J(p - \mathbf{q}) ^2 -  J(p) ^2 \right) \frac{1}{2\mu^4} \left( 1 - \frac{1}{2} e^{-\mu\Delta z} \right)^2$
(GLV) <sub>SUB</sub>	$\frac{N}{A_\perp} \frac{1}{d_A} C_2(R) C(R) (4\pi\alpha_s)^2 \int \rho(\Delta z) \int \frac{d^2\mathbf{q}}{(2\pi)^2} \left(  J(p - \mathbf{q}) ^2 -  J(p) ^2 \right) \frac{4}{(1 + \gamma)^2} \frac{1}{2\mu^4}$
(GLV + APL) <sub>SUB</sub>	$\frac{N}{A_\perp} \frac{1}{d_A} C_2(R) C(R) (4\pi\alpha_s)^2 \int \rho(\Delta z) \int \frac{d^2\mathbf{q}}{(2\pi)^2} \left(  J(p - \mathbf{q}) ^2 -  J(p) ^2 \right) \frac{4}{(1 + \gamma)^2} \frac{1}{2\mu^4} \left( 1 - \frac{1}{2} e^{-\mu\Delta z} \right)^2$

TABLE II:  $dN^{(1)}/d^3\vec{p}$  for different approximation schemes to momentum broadening considered in this work.

(fig. 1a). The matrix elements are combined via eq. (5), yielding the momentum broadening distribution, with the results summarized in table II. Notably the results from  $\text{Tr}\langle|\mathcal{M}_1|^2\rangle$  are the same as the results from  $\text{Re}(\text{Tr}\langle\mathcal{M}_0^*\mathcal{M}_2\rangle)$ , differing only by a crucial factor of  $\frac{1}{2}$  and a shift in the amplitude.

In the case of the (GLV + APL) corrections, the correction introduces  $(1 - \frac{1}{2}e^{-\mu\Delta z})^2$  as is expected from [48]. If one applies  $e^{-\mu\Delta z} \rightarrow 0$ , to APL, one recovers the original GLV result. Interestingly, the inclusion of the APL correction suggests there would be less broadening in small system sizes when  $\mu\Delta z$  is no longer  $\gg 1$ . The exponential correction factor will dominate and suppress the broadening compared to original GLV.

The sub-eikonal correction to  $dN^{(1)}/d^3\vec{p}$  takes the form  $4/(1 + \gamma)^2$ . The introduction of the  $\gamma$ -factor allows for broadening effects when  $\mathbf{q} \sim P^+$  and  $\gamma$  becomes  $< 1$ . The overall correction is proportional to  $1/\gamma^2$ , since  $\gamma \leq 1$  the correction becomes  $1/\gamma^2 \geq 1$ . The inclusion of the sub-eikonal correction suggests more broadening at large exchanged momentum compared to the initial incoming longitudinal momentum of the parton. In the eikonal limit when  $\mathbf{q} \ll P^+$ ,  $\gamma \rightarrow 1$  and one recovers the GLV result.

We also present a combined APL and sub-eikonal correction to GLV. The (GLV + APL)<sub>SUB</sub> calculation is done using the sub-eikonal kinematics which leads to the  $\gamma$ -factor, in the form  $4/(1 + \gamma)^2$ , which is the same as the purely sub-eikonal case. The (GLV + APL)<sub>SUB</sub> calculation also includes the APL terms  $(1 - \frac{1}{2}e^{-\mu\Delta z})^2$ . The combined result may be reduced to the individual corrections in the appropriate limits.

## VI. DISCUSSION AND NUMERICAL INVESTIGATION

To investigate the full impact of the (GLV+APL), (GLV)<sub>SUB</sub> and (GLV+APL)<sub>SUB</sub> corrections, we present a numerical analysis of the resulting momentum broadening distributions as a function of the broadened momentum  $\mathbf{p}$ . In all cases, we adopt the parameters  $\alpha_s = 0.3$ ,  $\mu_D = 0.5$  GeV, an initial parton momentum  $P^+ = 40$  GeV and a system size  $L = 4$  fm. The color factors used are  $C_F = 4/3$  for the quadratic Casimir of the fundamental representation,  $C_A = 3$  for the quadratic Casimir of the adjoint representation, and  $d_A = 8$  for the dimension of the adjoint representation. We do not present results for an incoming gluon, as they differ from the quark case only by an overall color factor, which cancels in the ratio.

To obtain the transverse momentum  $\mathbf{p}$  dependence we perform a double Fourier transform  $\mathbf{q} \rightarrow \mathbf{b} \rightarrow \mathbf{p}$ .

$$f(\mathbf{p}) = \int d^2\mathbf{b} F(\mathbf{b}) e^{i\mathbf{b}\cdot\mathbf{p}}, \quad (23)$$

$$F(\mathbf{b}) = \int \frac{d^2\mathbf{q}}{(2\pi)^2} f(\mathbf{q}) e^{-i\mathbf{q}\cdot\mathbf{b}} \quad (24)$$

Thus distribution becomes

$$\frac{dN^{(1)}}{d^3\vec{p}} = \frac{N}{A_\perp} \frac{1}{d_A} C_2(R) C(R) (4\pi\alpha_s)^2 f(\mathbf{p}). \quad (25)$$

The transverse momentum transfer cannot fall below the Debye scale, giving the infrared limit

$$\mathbf{p} \geq \mu_D.$$

For the sub-eikonal correction, the all-order factor  $\gamma$  must be real. Its maximum value  $\gamma = 1$  corresponds to the maximum allowed momentum transfer  $\mathbf{q}^{\max} = \sqrt{2}/2P^+$  and provides an UV limit. Thus, the physically relevant transverse-momentum domain is

$$\mu_D \leq \mathbf{p} \leq \frac{\sqrt{2}}{2} P^+. \quad (26)$$

The momentum broadening of the GLV model is plotted against the transverse momentum  $\mathbf{p}$  in fig. 2 where the plot may directly be compared to the results presented in Fig.3 of [45]. There is a suppression of the (GLV + APL) corrected distribution at low- $\mathbf{p}$ . At high- $\mathbf{p}$  the effect is more obvious where there is an enhancement of the sub-eikonal corrected curves.

To see the effects more clearly we plot the ratio of the the distribution with a correction to the standard GLV distribution in the bottom panel of fig. 2.

In fig. 2, the low- $\mathbf{p}$  limit, there is a clear divergence of the (GLV + APL) corrected distribution relative to GLV, leading to a steep fall-off near the lower bound  $\mu = \mu_D$ . At low- $\mathbf{p}$ , corresponding to small  $\mu$ , the correction term dominates and suppresses the GLV result. At high  $\mathbf{p}$ , when  $\mu$  is large, the APL correction tends to zero ( $e^{-\mu\Delta z} \rightarrow 0$ ), and the (GLV + APL) distribution converges to the original GLV result.

The GLV distribution with sub-eikonal corrections (GLV)<sub>SUB</sub> diverges from the GLV result in the high  $\mathbf{p}$  limit. In contrast, at low- $\mathbf{p}$ , the sub-eikonal correction tends to zero, and (GLV)<sub>SUB</sub> converges to GLV, consistent with  $\mathbf{q}/P^+ \ll 1$  and  $\gamma \rightarrow 1$ .

We also consider the combined APL and sub-eikonal correction (GLV+APL)<sub>SUB</sub>. In the low- $\mathbf{p}$  limit, this distribution approaches (GLV + APL), as the sub-eikonal correction becomes negligible. In the high- $\mathbf{p}$  limit, the distribution approaches (GLV)<sub>SUB</sub>, as the APL correction vanishes. Suggesting reduced broadening at low- $\mathbf{p}$  and enhanced broadening at high- $\mathbf{p}$  as compared to original GLV.

To investigate the effect of APL correction, we present fig. 3a. The two APL corrected distributions, (GLV + APL) and (GLV+APL)<sub>SUB</sub> are shown, relative to GLV for three different system sizes  $L$  ( $L = 1, 4, 10$  fm). After performing the integral over the distance between scattering centres  $\int d\Delta z$ , the APL corrections scale as  $\propto 1/(L\mu)$ . At low- $\mathbf{p}$ , which corresponds to small  $\mu$ , the APL corrections dominate, smaller  $L$  corresponds to a larger correction factor, while larger  $L$  reduces the correction and the result approaches GLV. At high- $\mathbf{p}$ , which correspond to large  $\mu$ , the APL corrections converge to GLV, and (GLV + APL)<sub>SUB</sub> converges to (GLV)<sub>SUB</sub>, consistent with  $1/(L\mu) \rightarrow 0$ .

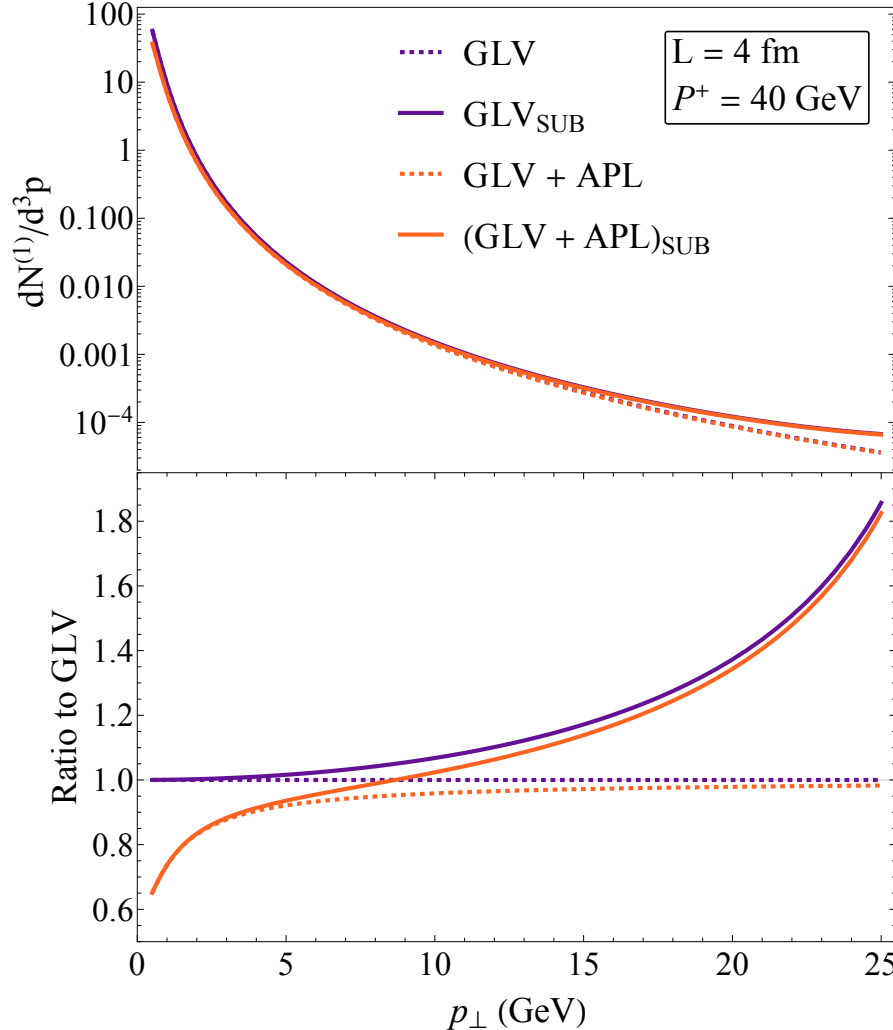


FIG. 2: The broadening distribution to first order in the opacity expansion  $d^{(1)}N/d^3\vec{p}$  is shown for three correction schemes— $(\text{GLV} + \text{APL})$ , sub-eikonal  $(\text{GLV})_{\text{SUB}}$ , and the combined correction  $(\text{GLV} + \text{APL})_{\text{SUB}}$ . Each corrected distribution is plotted both individually (top panel) and as a ratio to the unmodified GLV baseline (bottom panel), as a function of  $\mathbf{p}$  for fixed initial parton momentum  $P^+ = 40$  GeV and system size  $L = 4$  fm.

To investigate the effect of the sub-eikonal correction, we present fig. 3b. We plot the ratios of the two sub-eikonal corrected distributions  $(\text{GLV})_{\text{SUB}}$  and  $(\text{GLV} + \text{APL})_{\text{SUB}}$  to GLV as a function of  $\mathbf{p}$  for three different initial parton momenta  $P^+$  ( $P^+ = 7, 8, 10$  GeV). As discussed, the sub-eikonal corrections dominate at large  $\mathbf{p}$  as this is when the  $\gamma$ -factor can no longer be approximated as 1.

A smaller initial momentum  $P^+$  leads to larger corrections within the same  $\mathbf{p}$  range. The sub-eikonal terms become relevant more rapidly for smaller  $P^+$  because  $\mathbf{q}$  approaches  $P^+$  more quickly, causing  $\gamma$  to be less than 1 sooner. At low- $\mathbf{p}$ , the sub-eikonal corrections vanish as  $\mathbf{q}/P^+ \ll 1$  and  $\gamma \rightarrow 1$ . Thus,  $(\text{GLV})_{\text{SUB}}$  converges to GLV and  $(\text{GLV} + \text{APL})_{\text{SUB}}$  converges to  $(\text{GLV} + \text{APL})$  for all  $P^+$ , consistent with eikonal approximation  $\mathbf{q}/P^+ \ll 1$ .

To investigate the relationship between the APL and sub-eikonal corrections we present fig. 4a. The ratios of  $(\text{GLV} + \text{APL})$ ,  $(\text{GLV})_{\text{SUB}}$ , and  $(\text{GLV} + \text{APL})_{\text{SUB}}$  to the original GLV result as a function of  $L$ , with the exchanged momentum held fixed. The exchanged transverse momentum  $\mathbf{p}$  has been numerically integrated over the range specified in eq. (26). In the case of GLV and  $(\text{GLV})_{\text{SUB}}$ , which exhibit a linear  $L$  dependence through  $N/A_\perp = L/\lambda$ , taking the ratio removes the  $L$  dependence. Consequently, both GLV and  $(\text{GLV})_{\text{SUB}}$  ratios to GLV are constant as functions of  $L$ .

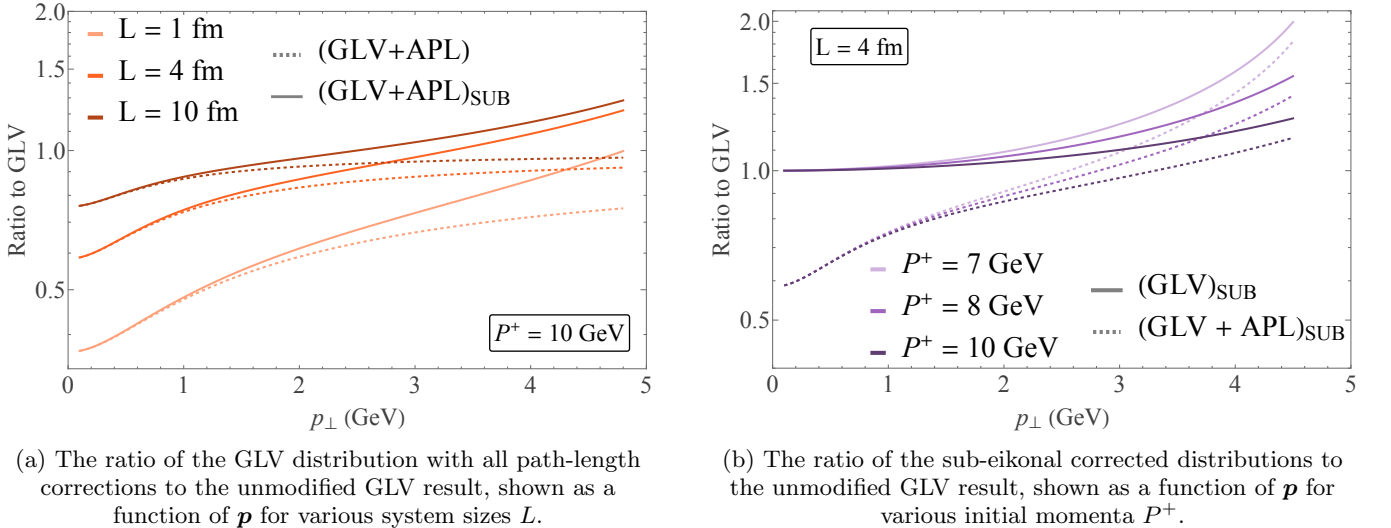


FIG. 3: The ratios of the various corrected broadening distributions — the all path-length–corrected (GLV + APL), the sub-eikonal corrected  $(\text{GLV})_{\text{SUB}}$ , and the combined all path-length and sub-eikonal corrected  $(\text{GLV} + \text{APL})_{\text{SUB}}$  distributions — to the standard GLV result are plotted as functions of  $\mathbf{p}$ . For the path-length–corrected case (a), results for different system sizes  $L = 1, 4, 10$  fm at fixed initial parton momentum  $P^+ = 10$  GeV are shown, while for the sub-eikonal case (b), results for different initial momenta  $P^+ = 7, 8, 10$  GeV at fixed system size  $L = 4$  fm are shown.

For the APL corrections, one observes that at large  $L$ , where the APL correction vanishes, the corresponding ratios converge to their respective baseline models. For small  $L$ , however, where the APL correction dominates, we observe a steep fall-off, indicating a suppression of the momentum broadening for small  $L$  compared to GLV and  $(\text{GLV})_{\text{SUB}}$ .

An interesting comparison is provided by  $(\text{GLV} + \text{APL})$  and  $(\text{GLV} + \text{APL})_{\text{SUB}}$ . Upon introducing the sub-eikonal correction to the APL contribution, we find that the sub-eikonal correction mitigates the suppression induced by the APL term and leads to an enhancement of the momentum broadening. Since the sub-eikonal correction reduces the APL contribution and becomes largely positive at  $\mathbf{p} \sim P^+$ , it may provide a possible resolution to the large negative corrections at high energies reported in [48].

Lastly, we present fig. 4b, which shows the momentum broadening distributions for  $(\text{GLV})_{\text{SUB}}$ ,  $(\text{GLV} + \text{APL})$ , and  $(\text{GLV} + \text{APL})_{\text{SUB}}$  as functions of  $P^+$ , with the system size held fixed. The exchanged transverse momentum  $\mathbf{p}$  has been numerically integrated over the range specified in eq. (26).

We observe that the  $(\text{GLV} + \text{APL})$  result lies below the GLV curve, indicating a reduction in momentum broadening when the APL correction is included. In contrast, the inclusion of sub-eikonal corrections enhances momentum broadening:  $(\text{GLV})_{\text{SUB}}$  lies above the GLV result for all values of  $P^+$ . These trends demonstrate that while the APL correction suppresses momentum broadening, the sub-eikonal correction has the opposite effect.

A key result is that when both corrections are included, the sub-eikonal contribution partially mitigates the suppression induced by the APL correction. This is reflected in the fact that  $(\text{GLV} + \text{APL})_{\text{SUB}}$  lies above  $(\text{GLV} + \text{APL})$  for all  $P^+$ . This behavior is consistent with the trends observed in fig. 2 and lends additional support to the view that sub-eikonal corrections may help alleviate the large negative contributions at high energies reported in [48].

Finally, we note that the sub-eikonal correction is particularly significant at lower values of  $P^+$ . In this regime,  $\mathbf{q} \sim P^+$  and the  $\gamma$ -factor satisfies  $\gamma \neq 1$ , enhancing the importance of sub-eikonal effects.

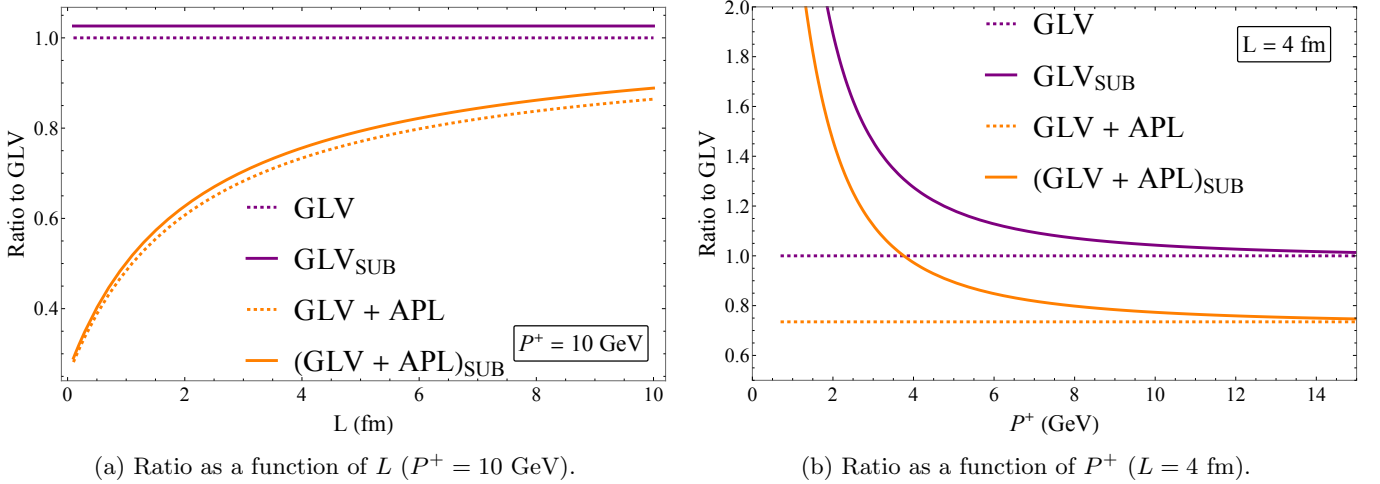


FIG. 4: The ratios of the various corrected broadening distributions — the all path-length-corrected (GLV + APL), the sub-eikonal corrected (GLV)<sub>SUB</sub>, and the combined all path-length and sub-eikonal corrected (GLV + APL)<sub>SUB</sub> distributions — to the standard GLV result are plotted as function of system size  $L$  in (a), for a fixed initial parton momentum  $P^+ = 10$  GeV. As a function of initial parton momentum  $P^+$  in (b), for a fixed system size  $L = 4$  fm.

## VII. CONCLUSION

We computed the momentum broadening distribution to first order in the opacity expansion,  $\frac{dN^{(1)}}{d^3\vec{p}}$ , using the GLV formalism, implementing (GLV + APL), (GLV)<sub>SUB</sub> and (GLV + APL)<sub>SUB</sub> corrections.

The APL correction leads to a suppression of the momentum broadening for low- $\vec{p}$  and the sub-eikonal correction leads to an enhancement of the momentum broadening at high- $\vec{p}$ . The sub-eikonal correction mitigates the effect of the APL correction, suggesting a possible solution to the large negative correction found in the radiative case.

This behavior is also reflected in the dependence on  $P^+$  and  $L$ : for all values considered, the inclusion of sub-eikonal corrections consistently increases the momentum broadening relative to the GLV baseline, whereas the APL correction leads to a systematic reduction compared to GLV.

The broadening results have the expected form associated with the GLV formalism and reduce to the standard GLV result in the appropriate limits. The results for the broadening distribution are valid for all system sizes,  $L$ , and up to initial parton momentum ( $\frac{1}{P^{+3}}$ ). If one wishes to extend the distribution to higher orders in  $P^+$ , one must take into account corrections to the source amplitude  $J(p)$  and additional double scattering diagrams that become relevant at  $\mathcal{O}(\frac{1}{P^{+4}})$ .

## Appendix A: Details of results calculated

In this section, we present a more detailed derivation of the results shown in table II. In particular, we show the GLV and (GLV)<sub>SUB</sub> calculations from the kinematical level as each uses a different set of kinematics. The (GLV + APL) and (GLV)<sub>SUB</sub> are obtained with the same kinematics as each of the non APL based results as is outlined in table I.

### Standard GLV calculation

#### Single Scattering

To compute the momentum broadening distribution we first compute  $\mathcal{M}_1$ , we evaluate the  $q_z$  integral analytically using the residue theorem. The integral to be computed is

$$I_1 = \int \frac{dq_z}{2\pi} \frac{1}{(p-q)^2 + i\epsilon} \frac{4\pi\alpha_s}{q_z^2 + \mu^2} e^{-iq_z\Delta z}. \quad (\text{A1})$$

Using  $(p - q)^2 + i\epsilon = -q_z^2 + \sqrt{2}P^+q_z + \mathbf{q}^2 + i\epsilon = -(q_z - q_z^{(+)})(q_z - q_z^{(-)}) + i\epsilon$  and  $q_z^2 + \boldsymbol{\mu}^2 = (q_z + i\boldsymbol{\mu})(q_z - i\boldsymbol{\mu})$ , we close the contour in the negative complex plane. The contributing poles are given by

$$q_z^{(1)} = -\frac{\sqrt{2}}{2} \frac{\mathbf{q}^2}{P^+} - i\epsilon, \quad (\text{A2})$$

$$q_z^{(2)} = -i\boldsymbol{\mu}. \quad (\text{A3})$$

The residues associated with each pole are

$$\text{Res}[I_1, q_z^{(1)}] = \lim_{q_z \rightarrow q_z^{(1)}} \frac{-1}{(p - q)^2 + i\epsilon} \frac{4\pi\alpha_s}{q_z^2 + \boldsymbol{\mu}^2} e^{-iq_z\Delta z} (q_z - q_z^{(1)}) \quad (\text{A4})$$

$$= \frac{-1}{(\frac{\sqrt{2}}{2} \frac{\mathbf{q}^2}{P^+} - \sqrt{2}P^+) (\frac{\sqrt{2}}{2} \frac{\mathbf{q}^2}{P^+})^2 + \boldsymbol{\mu}^2} e^{-i(-\frac{\sqrt{2}}{2} \frac{\mathbf{q}^2}{P^+})\Delta z}. \quad (\text{A5})$$

Since  $\mathbf{q} \ll P^+ \implies \frac{\mathbf{q}}{P^+} \ll 1 \implies \frac{\mathbf{q}^2}{P^+} \ll \mathbf{q} \ll P^+$ . We also have that  $\boldsymbol{\mu}^2 = \mathbf{q}^2 + \mu^2 \implies \boldsymbol{\mu} = \sqrt{\mathbf{q}^2 + \mu^2} = \mathbf{q}\sqrt{1 + \frac{\mu^2}{\mathbf{q}^2}} \approx \mathbf{q} \implies \frac{\mathbf{q}^2}{P^+} \ll \mathbf{q} \approx \boldsymbol{\mu}$ . Using these assumptions one has in standard GLV  $\frac{-\sqrt{2}}{2} \frac{\mathbf{q}^2}{P^+} - \sqrt{2}P^+ \approx -\sqrt{2}P^+$  and  $(\frac{\sqrt{2}}{2} \frac{\mathbf{q}^2}{P^+})^2 + \boldsymbol{\mu}^2 = (\frac{\sqrt{2}}{2} \frac{\mathbf{q}^2}{P^+} + i\boldsymbol{\mu})(\frac{\sqrt{2}}{2} \frac{\mathbf{q}^2}{P^+} - i\boldsymbol{\mu}) \approx (i\boldsymbol{\mu})(-i\boldsymbol{\mu}) = \boldsymbol{\mu}^2$ . Since  $\frac{\sqrt{2}}{2} \frac{\mathbf{q}^2}{P^+} \ll 1$  and  $e^{ix} \approx 1$  for  $x \ll 1$  therefore  $e^{i\frac{\sqrt{2}}{2} \frac{\mathbf{q}^2}{P^+}\Delta z} \approx 1$  so

$$\text{Res}[I_1, q_z^{(1)}] = \frac{1}{\sqrt{2}P^+} \frac{4\pi\alpha_s}{\boldsymbol{\mu}^2}. \quad (\text{A6})$$

The pole from the propagator gives,

$$\text{Res}[I_1, q_z^{(2)}] = \lim_{q_z \rightarrow q_z^{(2)}} \frac{1}{(p - q)^2 + i\epsilon} \frac{4\pi\alpha_s}{q_z^2 + \boldsymbol{\mu}^2} e^{-iq_z\Delta z} (q_z - q_z^{(2)}) \quad (\text{A7})$$

$$= \frac{-1}{(-i\boldsymbol{\mu} + \frac{\sqrt{2}}{2} \frac{\mathbf{q}^2}{P^+})(-i\boldsymbol{\mu} - \sqrt{2}P^+) (-2i\boldsymbol{\mu})} \frac{4\pi\alpha_s}{(-2i\boldsymbol{\mu})} e^{-\boldsymbol{\mu}\Delta z}. \quad (\text{A8})$$

We simplify using the arguments stated above. Since  $\mathbf{q} \ll P^+$  and  $\mathbf{q} \approx \boldsymbol{\mu} \implies -i\boldsymbol{\mu} - \sqrt{2}P^+ \approx -\sqrt{2}P^+$ . We also have that  $\frac{\mathbf{q}^2}{P^+} \ll \mathbf{q} \approx \boldsymbol{\mu} \implies -i\boldsymbol{\mu} + \frac{\sqrt{2}}{2} \frac{\mathbf{q}^2}{P^+} \approx -i\boldsymbol{\mu}$  and therefore we have that

$$\text{Res}[I_1, q_z^{(2)}] = \frac{-1}{(-i\boldsymbol{\mu})(-\sqrt{2}P^+)} \frac{4\pi\alpha_s}{(-2i\boldsymbol{\mu})} e^{-\boldsymbol{\mu}\Delta z} = \frac{-4\pi\alpha_s}{2\sqrt{2}P^+ \boldsymbol{\mu}^2} e^{-\boldsymbol{\mu}\Delta z}. \quad (\text{A9})$$

In the large separation distance approximation  $\boldsymbol{\mu}\Delta z \gg 1$ . Therefore  $e^{-\boldsymbol{\mu}\Delta z} \approx 0$  and one has

$$\text{Res}[I_1, q_z^{(2)}] = 0. \quad (\text{A10})$$

Using the sum of the residues the integral is given by,

$$I_1 = \frac{-i}{\sqrt{2}P^+} \frac{4\pi\alpha_s}{\boldsymbol{\mu}^2}. \quad (\text{A11})$$

Taking the complex conjugate, the single scattering contribution to the broadening distribution is therefore given by,

$$\text{Tr}\langle |\mathcal{M}_1|^2 \rangle = \frac{N}{A_\perp} \frac{1}{d_A} C_2(R) C(R) (4\pi\alpha_s)^2 \int \rho(\Delta z) \int \frac{d^2\mathbf{q}}{(2\pi)^2} |J(p - \mathbf{q})|^2 \frac{1}{2\boldsymbol{\mu}^4}. \quad (\text{A12})$$

### Double Scattering

The first integral we wish to compute is,

$$I_2 = \int \frac{dq_{1,z}}{2\pi} v(q_1) \frac{1}{(p - q_1 - q_2)^2 + i\epsilon} e^{-iq_{1,z}\Delta z}. \quad (\text{A13})$$

We make the substitution  $q_3 = q_1 + q_2$  and  $dq_3 = dq_1$ . Therefore the integral to be computed is,

$$I_2 = \int \frac{dq_{3,z}}{2\pi} \frac{4\pi\alpha_s}{\vec{q}_1^2 + \mu^2} \frac{1}{(p - q_3)^2 + i\epsilon} e^{-iq_{3,z}\Delta z}. \quad (\text{A14})$$

We observe that  $I_2$  takes the same form as the previous integral  $I_1$ . Therefore if we close the the contour in the lower half of the complex plane the poles from the propagator and potential that contribute are given by,

$$q_{1,z}^{(1)} = -\frac{\sqrt{2}}{2} \frac{\mathbf{q}_3^2}{P^+} - q_{2,z} - i\epsilon, \quad (\text{A15})$$

$$q_{1,z}^{(2)} = -i\mu_1, \quad (\text{A16})$$

where  $\mu_1^2 = \mathbf{q}_1^2 + \mu^2$ . Applying the same approximations as before

$$\text{Res}[I_2, q_{z,1}^{(1)}] = \frac{4\pi\alpha_s}{\sqrt{2}P^+} \frac{1}{q_{2,z}^2 + \mu_1^2}, \quad (\text{A17})$$

$$\text{Res}[I_2, q_{z,1}^{(2)}] = \frac{-4\pi\alpha_s}{2\sqrt{2}i\mu_1 P^+ (q_{2,z} - i\mu_1)} e^{-i(q_{2,z} - i\mu_1)\Delta z}. \quad (\text{A18})$$

In the large separation distance approximation  $\mu\Delta z \gg 1$ . Therefore  $e^{-\mu\Delta z} \approx 0$  and one has

$$\text{Res}[I_2, q_{z,2}^{(2)}] = 0. \quad (\text{A19})$$

The integral in eq. (A14) is then given by

$$I_2 = \frac{-i}{\sqrt{2}P^+} \frac{4\pi\alpha_s}{q_{2,z}^2 + \mu_1^2}. \quad (\text{A20})$$

Moving to the next integral,

$$I_3 = \int \frac{dq_{2,z}}{2\pi} \frac{4\pi\alpha_s}{q_{2,z}^2 + \mu_1^2} \frac{4\pi\alpha_s}{\vec{q}_2^2 + \mu^2} \frac{1}{(p - q_2)^2 + i\epsilon} e^{-iq_{2,z}\Delta z'}. \quad (\text{A21})$$

Where  $\Delta z' \equiv z_2 - z_1$ . We close the contour in the negative half of the complex plane, resulting in three poles:

$$q_{2,z}^{(1)} = -\frac{\sqrt{2}}{2} \frac{q_{2,z}^2}{P^+} - i\epsilon, \quad (\text{A22})$$

$$q_{2,z}^{(2)} = -i\mu_2, \quad (\text{A23})$$

$$q_{2,z}^{(3)} = -i\mu_1. \quad (\text{A24})$$

Computing the residues with the same approximations,

$$\text{Res}[I_3 I_2, q_{2,z}^{(1)}] = \frac{-i(4\pi\alpha_s)^2}{2\mu_1^2\mu_2^2 P^{+2}}. \quad (\text{A25})$$

$$\text{Res}[I_3 I_2, q_{2,z}^{(2)}] = \frac{i(4\pi\alpha_s)^2}{4P^{+2}\mu_1^2(\mu_2^2 - \mu_1^2)} e^{-\mu_1 \Delta z'} \quad (\text{A26})$$

In the contact limit  $z_2 \rightarrow z_1$ , so  $\Delta z' \rightarrow 0$

$$\text{Res}[I_3, q_{2,z}^{(3)}] = \frac{i(4\pi\alpha_s)^2}{4P^{+2}\mu_2^2(\mu_1^2 - \mu_2^2)} \quad (\text{A27})$$

Combining eq. (A20) and eq. (A21) gives

$$I_3 I_2 = \frac{-2\pi i}{2\pi} \sum_{j=1}^2 \text{Res}[I_3 I_2, q_z^{(j)}] \quad (\text{A28})$$

$$= \frac{-(4\pi\alpha_s)^2}{2P^{+2}} \left( \frac{1}{\mu_1^2\mu_2^2} - \frac{1}{2\mu_1^2(\mu_2^2 - \mu_1^2)} - \frac{1}{2\mu_2^2(\mu_1^2 - \mu_2^2)} \right) \quad (\text{A29})$$

$$= \frac{-(4\pi\alpha_s)^2}{2P^{+2}} \left( \frac{(\mu_2^2 - \mu_1^2)}{2\mu_1^2\mu_2^2(\mu_2^2 - \mu_1^2)} \right) = \frac{-(4\pi\alpha_s)^2}{4P^{+2}\mu_1^2\mu_2^2}. \quad (\text{A30})$$

Now we apply the average over the impact parameter as per our discussion in eq. (7). Which sets  $\mu_1 = \mu_2$  as well as  $J(p - \mathbf{q}_1 - \mathbf{q}_2) = J(p)$ .

$$I_3 I_2 = \frac{-(4\pi\alpha_s)^2}{4P^{+2}\mu^4}. \quad (\text{A31})$$

The non-interacting matrix, fig. 1a, is given by

$$\mathcal{M}_0^* = -ie^{-ipz_0} J^*(p). \quad (\text{A32})$$

The double scattering contribution to the broadening distribution is therefore given by

$$\text{Tr}\langle \mathcal{M}_2 \mathcal{M}_0^* \rangle = \frac{N}{A_\perp} \frac{1}{d_A} C_2(R) C(R) (4\pi\alpha_s)^2 \int \rho(\Delta z) \int \frac{d^2\mathbf{q}}{(2\pi)^2} \cdot |J(p)|^2 \frac{-1}{4\mu^4} \quad (\text{A33})$$

Crucially we note the result of the double scattering contribution differs from the result of the single scattering by a factor of  $-\frac{1}{2}$ . Since the double scattering term has an overall factor of 2 when calculating the broadening distribution cancels the factor of  $\frac{1}{2}$ , resulting in that the single and double scattering contributions only differs in a shift in the amplitude.

#### *The momentum broadening distribution*

Our result for the distribution eq. (5) is then

$$\frac{dN^{(1)}}{d^3\vec{p}} = \left( \frac{1}{d_T} \text{Tr}\langle |\mathcal{M}_1|^2 \rangle + \frac{2}{d_T} \text{Re} \text{Tr}\langle \mathcal{M}_2 \mathcal{M}_0^* \rangle \right) \quad (\text{A34})$$

$$= \frac{N}{A_\perp} \frac{1}{d_A} C_2(R) C(R) (4\pi\alpha_s)^2 \int \rho(\Delta z) \int \frac{d^2\mathbf{q}}{(2\pi)^2} \left( |J(p-\mathbf{q})|^2 \frac{1}{2\mu} + 2|J(p)|^2 \frac{-1}{4\mu^4} \right) \quad (\text{A35})$$

$$= \frac{N}{A_\perp} \frac{1}{d_A} C_2(R) C(R) (4\pi\alpha_s)^2 \int \rho(\Delta z) \int \frac{d^2\mathbf{q}}{(2\pi)^2} \left( |J(p-\mathbf{q})|^2 - |J(p)|^2 \right) \frac{1}{2\mu^4} \quad (\text{A36})$$

### (GLV + APL) calculation

To perform the APL calculation we use the same kinematics as in the GLV case. However we relax the large system size approximation. Meaning the residues in eq. (A10) and eq. (A19) are no longer 0.

#### Single scattering

The single scattering residue with the non-zero APL residues

$$\text{Res}[I_1, q_z] = \sum_{j=1}^2 \text{Res}[I_1, q_z^{(j)}] = \frac{4\pi\alpha_s}{\sqrt{2}P^+\mu^2} \left( 1 - \frac{1}{2} e^{-\mu\Delta z} \right) \quad (\text{A37})$$

Therefore the integral is given by

$$I_1 = \frac{-i(4\pi\alpha_s)}{\sqrt{2}P^+\mu^2} \left( 1 - \frac{1}{2} e^{-\mu\Delta z} \right). \quad (\text{A38})$$

The single scattering contribution is given by

$$\text{Tr}\langle |\mathcal{M}_1|^2 \rangle = \frac{N}{A_\perp} \frac{1}{d_A} C_2(R) C(R) (4\pi\alpha_s)^2 \int \rho(\Delta z) \int \frac{d^2\mathbf{q}}{(2\pi)^2} \frac{1}{2\mu^4} \left( 1 - \frac{1}{2} e^{-\mu\Delta z} \right)^2. \quad (\text{A39})$$

#### Double scattering

The residues are once again the same as the GLV case, but with eq. (A19) no longer 0.

$$\text{Res}[I_2, q_{2,z}] = \sum_{j=1}^2 \text{Res}[I_2, q_{2,z}^{(j)}] \quad (\text{A40})$$

$$= \frac{4\pi\alpha_s}{\sqrt{2}P^+(q_{2,z} - i\mu_1)} \left( \frac{1}{q_{2,z} + i\mu_1} - \frac{e^{-i(q_{2,z} - i\mu_1)\Delta z}}{2i\mu_1} \right) \quad (\text{A41})$$

$$I_2 = \frac{-2\pi i}{2\pi} \text{Res}[I_2, q_{2,z}] \quad (\text{A42})$$

$$= \frac{-i(4\pi\alpha_s)}{\sqrt{2}P^+(q_{2,z} - i\mu_1)} \left( \frac{1}{q_{2,z} + i\mu_1} - \frac{e^{-i(q_{2,z} - i\mu_1)\Delta z}}{2i\mu_1} \right) \quad (\text{A43})$$

Moving to the  $I_3$ -integral the poles are the same as before as in eqs. (A22) to (A24).

$$\text{Res}[I_3, q_{2,z}^{(1)}] = \frac{(4\pi\alpha_s)}{\sqrt{2}\mu_1^2\mu_2^2 P^+} (1 - \frac{1}{2}e^{-\mu_1\Delta z}), \quad (\text{A44})$$

$$\text{Res}[I_3, q_{2,z}^{(2)}] = \frac{-(4\pi\alpha_s)}{2\sqrt{2}P^+\mu_1^2(\mu_2^2 - \mu_1^2)} e^{-\mu_1\Delta z'}, \quad (\text{A45})$$

$$\text{Res}[I_3, q_{2,z}^{(3)}] = \frac{(4\pi\alpha_s)}{2\sqrt{2}P^+\mu_2^2(\mu_2 + \mu_1)} \left( \frac{1}{\mu_2 - \mu_1} + \frac{e^{-(\mu_1 + \mu_2)\Delta z}}{2\mu_1} \right) e^{-\mu_2\Delta z'}. \quad (\text{A46})$$

Grouping the relevant terms together and applying the contact limit  $\Delta z' \rightarrow 0$ ,

$$I_3 = \frac{-i(4\pi\alpha_s)}{\sqrt{2}P^+} \left( \left[ \frac{1}{\mu_1^2\mu_2^2} - \frac{1}{2\mu_1^2(\mu_2^2 - \mu_1^2)} + \frac{1}{2\mu_2^2(\mu_2^2 - \mu_1^2)} \right] - \frac{1}{2} \frac{1}{\mu_1^2\mu_2^2} e^{-\mu_1\Delta z} + \frac{1}{4\mu_1\mu_2^2(\mu_2 + \mu_1)} e^{-(\mu_1 + \mu_2)\Delta z} \right). \quad (\text{A47})$$

The bracket without any exponential term simplifies as

$$[\dots] = \frac{1}{2\mu_1^2\mu_2^2}. \quad (\text{A48})$$

Therefore applying the contact limit (eq. (7)) one has,

$$I_3 I_2 = \frac{-(4\pi\alpha_s)^2}{4P^{+2}\mu^4} \left( 1 - \frac{1}{2}e^{-\mu\Delta z} \right)^2 \quad (\text{A49})$$

The double scattering contribution to the broadening distribution is therefore given by

$$\text{Tr}\langle \mathcal{M}_2 \mathcal{M}_0^* \rangle = \frac{N}{A_\perp} \frac{1}{d_A} C_2(R) C(R) (4\pi\alpha_s)^2 \int \frac{d^2\mathbf{q}}{(2\pi)^2} |J(p)|^2 \frac{-1}{4\mu^4} \left( 1 - \frac{1}{2}e^{-\mu\Delta z} \right)^2. \quad (\text{A50})$$

#### *The momentum broadening distribution*

Computing the momentum broadening distribution as per eq. (5), one has

$$\frac{dN^{(1)}}{d^3\vec{p}} = \left( \frac{1}{d_T} \text{Tr}\langle |\mathcal{M}_1|^2 \rangle + \frac{2}{d_T} \text{Re} \text{Tr}\langle \mathcal{M}_2 \mathcal{M}_0^* \rangle \right) \quad (\text{A51})$$

$$= \frac{N}{A_\perp} \frac{1}{d_A} C_2(R) C(R) (4\pi\alpha_s)^2 \int \rho(\Delta z) \int \frac{d^2\mathbf{q}}{(2\pi)^2} \left( |J(p - \mathbf{q})|^2 \frac{1}{2\mu} \left( 1 - \frac{1}{2}e^{-\mu\Delta z} \right)^2 \right. \quad (\text{A52})$$

$$\left. + 2|J(p)|^2 \frac{-1}{4\mu^4} \left( 1 - \frac{1}{2}e^{-\mu\Delta z} \right)^2 \right) \quad (\text{A53})$$

$$= \frac{N}{A_\perp} \frac{1}{d_A} C_2(R) C(R) (4\pi\alpha_s)^2 \int \rho(\Delta z) \int \frac{d^2\mathbf{q}}{(2\pi)^2} \left( |J(p - \mathbf{q})|^2 - |J(p)|^2 \right) \frac{1}{2\mu^4} \left( 1 - \frac{1}{2}e^{-\mu\Delta z} \right)^2 \quad (\text{A54})$$

We note that the double scattering result differs from the single scattering result by a factor of  $-\frac{1}{2}$ . This is crucial for the factorization and to preserve unitarity.

### (GLV)<sub>SUB</sub> calculation

In this section we present the calculation of the (GLV)<sub>SUB</sub> result. Crucially in the case of the SUB corrections we use a different set of kinematics as is outlined in table I. To see the effect of the sub-eikonal kinematics we use the propagator. For a parton on shell

$$(p - q)^2 + i\epsilon = M^2, \quad (\text{A55})$$

$$p^2 - 2pq + q^2 + i\epsilon = M^2, \quad (\text{A56})$$

$$-2pq + q^2 + i\epsilon = 0. \quad (\text{A57})$$

In the updated light-cone coordinates one has

$$p \cdot q = -q_z^2 - \frac{\sqrt{2}}{2} P^+ q_z - \mathbf{q}^2, \quad (\text{A58})$$

$$q^2 = -q_z^2 - \mathbf{q}^2. \quad (\text{A59})$$

substituting eqs. (A58) and (A59) into eq. (A57), one has

$$q_z^2 + \sqrt{2} P^+ q_z + \mathbf{q}^2 + i\epsilon = 0. \quad (\text{A60})$$

Applying the quadratic formula one has,

$$q_z^\pm = -\frac{\sqrt{2}}{2} P^+ (1 \pm \gamma) \pm i\epsilon = \beta^\pm, \quad (\text{A61})$$

where  $\gamma \equiv \sqrt{1 - \frac{2\mathbf{q}^2}{P^{+2}}}$ .

If one Taylor expands  $\beta^\pm$  to leading order one recovers the familiar GLV result  $q_z^+ = -\sqrt{2} P^+$  and  $q_z^- = -\frac{\sqrt{2}}{2} \frac{\mathbf{q}^2}{P^+}$ . By defining the  $\gamma$ -factor one encodes additional sub-eikonal terms for each pole of the propagator. Therefore the propagator factorizes as

$$(p - q)^2 + i\epsilon = (q_z - \beta^+)(q_z + \beta^+). \quad (\text{A62})$$

#### Single scattering

Closing the contour in the negative complex plane the contributing poles are

$$q_z^{(1)} = \beta^-, \quad (\text{A63})$$

$$q_z^{(2)} = -i\mu. \quad (\text{A64})$$

with residues

$$\text{Res}[I_1, q_z^{(1)}] = \lim_{q_z \rightarrow q_z^{(1)}} \frac{1}{(p - q)^2 + i\epsilon} \frac{4\pi\alpha_s}{(q_z^2 + \mu^2)} e^{-iq_z \Delta z} (q_z - q_z^{(1)}) \quad (\text{A65})$$

$$= \lim_{q_z \rightarrow q_z^{(1)}} \frac{1}{(q_z - \beta^-)(q_z - \beta^+)} \frac{4\pi\alpha_s}{(q_z^2 + \mu^2)} e^{-iq_z \Delta z} \times (q_z - \beta^-) \quad (\text{A66})$$

$$= \frac{4\pi\alpha_s}{(\beta^- - \beta^+)(\beta^- - i\mu)(\beta^+ + i\mu)} e^{-i\beta^- \Delta z}, \quad (\text{A67})$$

and

$$\text{Res}[I_1, q_z^{(2)}] = \lim_{q_z \rightarrow q_z^{(2)}} \frac{1}{(p-q)^2 + i\epsilon} \frac{4\pi\alpha_s}{(q_z^2 + \mu^2)} e^{-iq_z\Delta z} (q_z - q_z^{(2)}) \quad (\text{A68})$$

$$= \lim_{q_z \rightarrow q_z^{(2)}} \frac{1}{(q_z - \beta^-)(q_z - \beta^+)} \frac{4\pi\alpha_s}{(q_z + i\mu)(q_z - i\mu)} e^{-iq_z\Delta z} \times \frac{(q_z + i\mu)}{(q_z - i\mu)} \quad (\text{A69})$$

$$= \frac{i4\pi\alpha_s}{2\mu(i\mu + \beta^-)(i\mu + \beta^+)} e^{-\mu\Delta z}. \quad (\text{A70})$$

Now, since we are only performing a sub-eikonal correction we apply the large separation distance approximation and thus neglecting the path length for now,  $\text{Res}[I_1, q_z^{(2)}] = 0$  since  $e^{-\mu\Delta z} \rightarrow 0$  for  $\mu\Delta z \gg 1$ ,

$$I_1 = \frac{-2\pi i}{2\pi} \sum_{j=1}^2 \text{Res}[I_1, q_{2,z}^{(j)}] \quad (\text{A71})$$

$$= \frac{-2\pi i}{2\pi} (\text{Res}[I_1, q_z^{(1)}] + \text{Res}[I_1, q_z^{(2)}]) \quad (\text{A72})$$

$$= \frac{-i4\pi\alpha_s}{(\beta^- - \beta^+)(\beta^- - i\mu_\perp)(\beta^- + i\mu_\perp)} e^{-i\beta^-\Delta z}. \quad (\text{A73})$$

Now,  $e^{-i\beta^-\Delta z} \approx 1$  as  $\Delta z\beta^- \ll 1$ .  $\beta^-$  is still of the order  $\frac{q^2}{P^+}$  and therefore, as is pointed out in [22],  $\frac{\Delta z q^2}{P^+} \ll 1$  to preserve unitarity, so one has  $\Delta z\beta^- \ll 1$ . Also, the exponential factor will be 1 when taking the product with the complex conjugate. Thus the integral takes the form

$$I_1 = \frac{-i4\pi\alpha_s}{(\beta^- - \beta^+)(\beta^- - i\mu_\perp)(\beta^- + i\mu_\perp)}. \quad (\text{A74})$$

The single scattering contribution to the broadening distribution is given by

$$\text{Tr}\langle|\mathcal{M}_1|^2\rangle = \frac{N}{A_\perp} C_2(R) C(R) (4\pi\alpha_s)^2 \int \rho(\Delta z) \int \frac{d^2\mathbf{q}_\perp}{(2\pi)^2} |J(p - \mathbf{q}_\perp)|^2 P^{+2} \left[ \frac{1}{(\beta^- - \beta^+)^2 (\beta^- - i\mu_\perp)^2 (\beta^- + i\mu_\perp)^2} \right]. \quad (\text{A75})$$

At this point it is important to note that the eikonal correction has shown up in two ways. First through a scaling type correction  $P^+ \rightarrow \beta^+$ , and  $\frac{q^2}{P^+} \rightarrow \beta^-$ , where the inclusion of the  $\gamma$ -factor encodes sub-eikonal corrections to each pole. The other form is through additional terms such as  $\mu^2 \rightarrow \mu^2 + \beta^{-2}$ . These additional terms must still be simplified as keeping such additional terms results in a unitarity violation. Thus the result for  $\text{Tr}\langle|\mathcal{M}_1|^2\rangle$  consistent with unitarity is

$$\text{Tr}\langle|\mathcal{M}_1|^2\rangle = \frac{N}{A_\perp} C_2(R) C(R) (4\pi\alpha_s)^2 \int \rho(\Delta z) \int \frac{d^2\mathbf{q}_\perp}{(2\pi)^2} |J(p - \mathbf{q}_\perp)|^2 P^{+2} \left[ \frac{1}{\beta^{+2} \mu^4} \right] \quad (\text{A76})$$

### Double scattering

Recall the first integral we wish to compute

$$I_2 = \int \frac{dq_{3,z}}{2\pi} \frac{4\pi\alpha_s}{q_z^2 + \mu_1^2} \frac{1}{(p - q_3)^2 + i\epsilon} e^{-iq_{3,z}\Delta z}. \quad (\text{A77})$$

This integral takes the same form as  $I_1$ . We introduce

$$\beta_i^\pm = -\frac{\sqrt{2}}{2} P^+ \left( 1 \pm \gamma_i \right) \pm i\epsilon, \quad (\text{A78})$$

$$\gamma_i = \sqrt{1 - \frac{2q_i^2}{P^{+2}}}. \quad (\text{A79})$$

and therefore

$$I_2 = \frac{-i4\pi\alpha_s}{(\beta_3^- - \beta_3^+)(q_{2,z}^2 + \mu_1^2)}. \quad (\text{A80})$$

For  $I_3$ ,

$$I_3 = \int \frac{dq_{2,z}}{2\pi} \left( \frac{-i4\pi\alpha_s}{(\beta_3^- - \beta_3^+)(q_{2,z}^2 + \mu_1^2)} \right) \frac{1}{(p - q_2)^2 + i\epsilon} \frac{4\pi\alpha_s}{q_{2,z}^2 + \mu_2^2} e^{-iq_{2,z}\Delta z'}. \quad (\text{A81})$$

The poles are

$$q_{2,z}^{(1)} = -i\mu_2, \quad (\text{A82})$$

$$q_{2,z}^{(2)} = -\beta_2^-, \quad (\text{A83})$$

$$q_{2,z}^{(3)} = -\beta_3^- - i\mu_1. \quad (\text{A84})$$

Therefore the residues

$$\text{Res}[I_3, q_{2,z}^{(1)}] = \lim_{q_{2,z} \rightarrow q_{2,z}^{(1)}} \left( \frac{-i4\pi\alpha_s}{(\beta_3^- - \beta_3^+)[(\beta_3^- - q_{2,z})^2 + \mu_1^2]} e^{-i\beta_3^- \Delta z} + \frac{4\pi\alpha_s}{2\mu_1(q_{2,z} - i\mu_1 - \beta_3^-)(q_{2,z} - i\mu_1 - \beta_3^+)} \right. \quad (\text{A85})$$

$$\left. e^{-i(-i\mu_1 + q_{2,z})\Delta z} \right) \frac{1}{(q_{2,z} - \beta_2^-)(q_{2,z} - \beta_2^+)} \frac{4\pi\alpha_s}{(q_{2,z} - i\mu_2)(q_{2,z} + i\mu_2)} e^{-iq_{2,z}\Delta z'} \frac{(q_{2,z} + i\mu_2)}{(q_{2,z} - i\mu_2)} \quad (\text{A86})$$

$$= \left( \frac{-i4\pi\alpha_s}{(\beta_3^- - \beta_3^+)[(\beta_3^- + i\mu_2)^2 + \mu_1^2]} e^{-i\beta_3^- \Delta z} \right. \quad (\text{A87})$$

$$\left. + \frac{-4\pi\alpha_s}{2\mu_1(-i\mu_2 - i\mu_1 - \beta_3^-)(-i\mu_2 - i\mu_1 - \beta_3^+)} e^{-i(-i\mu_1 + -i\mu_2)\Delta z} \right) \quad (\text{A88})$$

$$\frac{4\pi\alpha_s}{(-2i\mu_2)(-i\mu_2 - \beta_2^-)(-i\mu_2 - \beta_2^+)} e^{-i(-i\mu_2)\Delta z'}. \quad (\text{A89})$$

Since we are computing only the sub-eikonal correction we take  $e^{-\mu\Delta z} \rightarrow 0$ ,  $e^{-\mu\Delta z'} \rightarrow 1$  and as argued before  $e^{-i\beta^- \Delta z} \rightarrow 1$ .

$$\text{Res}[I_3, q_{2,z}^{(1)}] = \frac{(4\pi\alpha_s)^2}{(\beta_3^- - \beta_3^+)[(\beta_3^- + i\mu_2)^2 + \mu_1^2](2\mu_2)(i\mu_2 + \beta_2^-)(i\mu_2 + \beta_2^+)} \quad (\text{A90})$$

and

$$\text{Res}[I_3, q_{2,z}^{(2)}] = \lim_{q_{2,z} \rightarrow q_{2,z}^{(2)}} \left( \frac{-i4\pi\alpha_s}{(\beta_3^- - \beta_3^+)[(\beta_3^- - q_{2,z})^2 + \mu_1^2]} e^{-i\beta_3^- \Delta z} + \frac{4\pi\alpha_s}{2\mu_1(q_{2,z} - i\mu_1 - \beta_3^-)(q_{2,z} - i\mu_1 - \beta_3^+)} \right. \quad (\text{A91})$$

$$\left. e^{-i(-i\mu_1 + q_{2,z})\Delta z} \right) \frac{1}{(q_{2,z} - \beta_2^-)(q_{2,z} - \beta_2^+)} \frac{4\pi\alpha_s}{(q_{2,z} - i\mu_2)(q_{2,z} + i\mu_2)} e^{-iq_{2,z}\Delta z'} \frac{(q_{2,z} + \beta_2^-)}{(q_{2,z} - \beta_2^-)} \quad (\text{A92})$$

$$= \left( \frac{-i4\pi\alpha_s}{(\beta_3^- - \beta_3^+)[(\beta_3^- - \beta_2^-)^2 + \mu_1^2]} e^{-i\beta_3^- \Delta z} + \frac{4\pi\alpha_s}{2\mu_1(\beta_2^- - i\mu_1 - \beta_3^-)(\beta_2^- - i\mu_1 - \beta_3^+)} \right. \quad (\text{A93})$$

$$\left. e^{-i(-i\mu_1 + \beta_2^-)\Delta z} \right) \frac{4\pi\alpha_s}{(\beta_2^- - \beta_2^+)(\beta_2^- - i\mu_2)(\beta_2^- + i\mu_2)} e^{-i(\beta_2^-)\Delta z'} \quad (\text{A94})$$

Applying the same simplifications.

$$\text{Res}[I_3, q_{2,z}^{(2)}] = \frac{-i(4\pi\alpha_s)^2}{(\beta_3^- - \beta_3^+)[(\beta_3^- - \beta_2^-)^2 + \mu_1^2](\beta_2^- - \beta_2^+)(\beta_2^- + \mu_2^2)} \quad (\text{A95})$$

and

$$\text{Res}[I_3, q_{2,z}^{(3)}] = \lim_{q_{2,z} \rightarrow q_{2,z}^{(3)}} \left( \frac{-i4\pi\alpha_s}{(\beta_3^- - \beta_3^+)(q_{2,z} - \beta_3^- + i\mu_1)(q_{2,z} - \beta_3^- - i\mu_1)} e^{-i\beta_3^- \Delta z} \right. \quad (\text{A96})$$

$$+ \frac{4\pi\alpha_s}{2\mu_1(q_{2,z} - i\mu_1 - \beta_3^-)(q_{2,z} - i\mu_1 - \beta_3^+)} e^{-i(-i\mu_1 + q_{2,z})\Delta z} \quad (\text{A97})$$

$$\frac{1}{(q_{2,z} - \beta_2^-)(q_{2,z} - \beta_2^+)} \frac{4\pi\alpha_s}{(q_{2,z} - i\mu_2)(q_{2,z} + i\mu_2)} e^{-iq_{2,z}\Delta z'} \frac{(q_{2,z} - \beta_3^- + i\mu_1)}{(\beta_3^- - i\mu_1 - \beta_2^+)} \quad (\text{A98})$$

$$= \frac{(4\pi\alpha_2)^2}{2\mu_1(\beta_3^- - \beta_3^+)(\beta_3^- - i\mu_1 - \beta_2^-)(\beta_3^- - i\mu_1 - \beta_2^+)(\beta_3^- - i\mu_1 - i\mu_2)(\beta_3^- - i\mu_1 + i\mu_2)} \quad (\text{A99})$$

$$e^{-i\beta_3^- \Delta z} e^{-i(\beta_3^- - i\mu_1)\Delta z'} \quad (\text{A100})$$

Applying the same simplifications

$$\text{Res}[I_3, q_{2,z}^{(3)}] = \frac{(4\pi\alpha_2)^2}{2\mu_1(\beta_3^- - \beta_3^+)(\beta_3^- - i\mu_1 - \beta_2^-)(\beta_3^- - i\mu_1 - \beta_2^+)(\beta_3^- - i\mu_1 - i\mu_2)(\beta_3^- - i\mu_1 + i\mu_2)}. \quad (\text{A101})$$

Now we need to add the residues to find  $I_3$ . One can see at this point the cross terms will be very complicated. The sub-eikonal correction manifests in two ways. Namely through rescaling and additional terms,

$$P^+ \rightarrow \beta^+, \quad (\text{A102})$$

$$\mu \rightarrow \mu + \beta^-. \quad (\text{A103})$$

The additional terms present a problem as one can clearly see the structure is not consistent from  $\mathcal{M}_1$  to  $\mathcal{M}_2$ , resulting in not factoring like  $J(\mathbf{p} - \mathbf{q})f(\mathbf{q}) - J(\mathbf{p})f(\mathbf{q}) = (J(\mathbf{p} - \mathbf{q}) - J(\mathbf{q}))f(\mathbf{q})$ . However if we focus on the rescaling part of the correction. We preserve  $P^+ \rightarrow \beta^+$  i.e. incorporating the  $\gamma$ -factor but dropping additional terms the residues become

$$\text{Res}[I_3, q_{2,z}^{(1)}] = \frac{(4\pi\alpha_s)^2}{(-\beta_3^+)(\mu_1^2 - \mu_2^2)(2\mu_2)(i\mu_2)(\beta_2^+)}, \quad (\text{A104})$$

$$\text{Res}[I_3, q_{2,z}^{(2)}] = \frac{-i(4\pi\alpha_s)^2}{(-\beta_3^+)(\mu_1^2)(-\beta_2^+)(\mu_2^2)}, \quad (\text{A105})$$

$$\text{Res}[I_3, q_{2,z}^{(3)}] = \frac{(4\pi\alpha_2)^2}{2\mu_1(-\beta_3^+)(-i\mu_1)(-\beta_2^+)(\mu_2^2 - \mu_1^2)}, \quad (\text{A106})$$

and therefore

$$I_3 = -i \sum_{j=1}^3 \text{Res}[I_3, q_{2,z}^{(j)}] = \frac{-(4\pi\alpha_s)^2}{2\mu_1^2\mu_2^2\beta_3^+\beta_2^+} \quad (\text{A107})$$

Now, if one applies the averaging over the impact parameter, one has

$$I_3 = \frac{-(4\pi\alpha_s)^2}{2\mu^4\beta^{+2}}. \quad (\text{A108})$$

Crucially, one has the factor of  $\frac{1}{2}$ .

$$\text{Tr}\langle \mathcal{M}_2 \mathcal{M}_0^* \rangle = \frac{N}{A_\perp} C_2(R) C(R) (4\pi\alpha_s)^2 \int \rho(\Delta z) \int \frac{d^2 \mathbf{q}_\perp}{(2\pi)^2} |J(p)|^2 P^{+2} \left[ -\frac{1}{2\beta^{+2}\mu^4} \right] \quad (\text{A109})$$

#### *The momentum broadening distribution*

The broadening distribution as per eq. (5) is therefore given by

$$\frac{dN^{(1)}}{d^3 \vec{p}} = \left( \frac{1}{d_T} \text{Tr}\langle |\mathcal{M}_1|^2 \rangle + \frac{2}{d_T} \text{Re} \text{Tr}\langle \mathcal{M}_2 \mathcal{M}_0^* \rangle \right) \quad (\text{A110})$$

$$= \frac{N}{A_\perp} \frac{1}{d_A} C_2(R) C(R) (4\pi\alpha_s)^2 \int \rho(\Delta z) \int \frac{d^2 \mathbf{q}}{(2\pi)^2} P^{+2} \left( |J(p - \mathbf{q})|^2 \frac{1}{\beta^{+2}\mu} + 2|J(p)|^2 \frac{-1}{2\beta^{+2}\mu^4} \right) \quad (\text{A111})$$

$$= \frac{N}{A_\perp} \frac{1}{d_A} C_2(R) C(R) (4\pi\alpha_s)^2 \int \rho(\Delta z) \int \frac{d^2 \mathbf{q}}{(2\pi)^2} P^{+2} \left( |J(p - \mathbf{q})|^2 - |J(p)|^2 \right) \frac{1}{\beta^{+2}\mu^4} \quad (\text{A112})$$

Simplifying, one has the substitution

$$\beta^{+2} = \frac{1}{2} P^{+2} (1 + \gamma)^2. \quad (\text{A113})$$

Therefore the double scattering contribution to the broadening is

$$\frac{dN^{(1)}}{d^3 \vec{p}} = \frac{N}{A_\perp} \frac{1}{d_A} C_2(R) C(R) (4\pi\alpha_s)^2 \int \rho(\Delta z) \int \frac{d^2 \mathbf{q}}{(2\pi)^2} \left( |J(p - \mathbf{q})|^2 - |J(p)|^2 \right) \left( \frac{4}{(1 + \gamma)^2} \frac{1}{2\mu^4} \right) \quad (\text{A114})$$

#### **(GLV + APL)<sub>SUB</sub> calculation**

Now we wish to look at the combined result of both the Sub-eikonal and All-Path-Length results. The full residues are already calculated in the previous section. Now we shall proceed to keep the additional path length terms  $\propto e^{\mu\Delta z}$  with the new scaling correction  $\beta^+$ .

#### *Single Scattering*

The residues are the same as before. We apply  $i\mu \pm \beta^- \rightarrow i\mu$  which is needed for unitarity. But we preserve the sub-eikonal correction by including the  $\gamma$ -factor through  $\beta^+$ . Now  $e^{-i\beta^-\Delta z} \approx 1$  as  $\beta^- \ll 1$  and  $\frac{\Delta z \mathbf{q}^2}{P^+} \ll 1$  is required to preserve unitarity. Therefore the residues become

$$\text{Res}[I_1, q_z^{(1)}] = \frac{-4\pi\alpha_s}{\beta^+\mu^2}, \quad (\text{A115})$$

and

$$\text{Res}[I_1, q_z^{(2)}] = \frac{4\pi\alpha_s}{2\beta^+\mu^2} e^{-\mu\Delta z}. \quad (\text{A116})$$

Notably we have the new residue of  $q_z^{(2)}$  which no longer 0 and introduces the path length factor  $e^{-\mu\Delta z}$ .

$$I_1 = -i \sum \text{Res} = \frac{i(4\pi\alpha_s)}{\beta^+ \mu} \left( 1 - \frac{1}{2} e^{-\mu\Delta z} \right) \quad (\text{A117})$$

Therefore

$$\text{Tr} \langle |\mathcal{M}_1|^2 \rangle = \frac{N}{A_\perp} C_2(R) C(R) (4\pi\alpha_s)^2 \int \rho(\Delta z) \int \frac{d^2 \mathbf{q}_\perp}{(2\pi)^2} |J(p - \mathbf{q}_\perp)|^2 P^{+2} \left[ \frac{1}{\beta^{+2} \mu^4} \left( 1 - \frac{1}{2} e^{-\mu\Delta z} \right)^2 \right] \quad (\text{A118})$$

### Double Scattering

Applying the same idea for to the double scattering residues.

$$\text{Res}[I_3, q_{2,z}^{(1)}] = \left( \frac{1}{\beta_3^+ (\mu_1^2 - \mu_2^2)} + \frac{1}{2\mu_1 \beta_3^+ (\mu_1 + \mu_2)} e^{-(\mu_1 + \mu_2)\Delta z} \right) \frac{i(4\pi\alpha_s)^2}{2\beta_2^+ \mu_2^2}, \quad (\text{A119})$$

$$\text{Res}[I_3, q_{2,z}^{(2)}] = \left( \frac{1}{\beta_3^+ \mu_1^2} - \frac{1}{2\beta_3^+ \mu_1^2} e^{-\mu_1 \Delta z} \right) \frac{-i(4\pi\alpha_s)^2}{\mu_2^2 \beta_2^+}, \quad (\text{A120})$$

$$\text{Res}[I_3, q_{2,z}^{(3)}] = \frac{i(4\pi\alpha_s)^2}{2\mu_1^2 \beta_2^+ \beta_3^+ (\mu_2^2 - \mu_1^2)}. \quad (\text{A121})$$

The integral is given by

$$I_3 = -i \sum_{j=1}^3 \text{Res}[I_3, q_{2,z}^{(j)}] \quad (\text{A122})$$

$$(\text{A123})$$

Adding the constant terms (terms without  $e^{-\mu\Delta z}$  factors).

$$\text{Constant} \left( \sum \text{Res} \right) = \frac{i(4\pi\alpha_s)^2}{2\beta_2^+ \beta_3^+ \mu_2^2 (\mu_1^2 - \mu_2^2)} + \frac{-i(4\pi\alpha_s)^2}{\beta_2^+ \beta_3^+ \mu_1^2 \mu_2^2} + \frac{i(4\pi\alpha_s)^2}{2\beta_2^+ \beta_3^+ \mu_1^2 (\mu_2^2 - \mu_1^2)} \quad (\text{A124})$$

$$= \frac{-i(4\pi\alpha_s)^2}{2\beta_2^+ \beta_3^+ \mu_1^2 \mu_2^2} \quad (\text{A125})$$

The full residue is therefore

$$\sum \text{Res} = \frac{-i(4\pi\alpha_s)^2}{2\beta_2^+ \beta_3^+ \mu_1^2 \mu_2^2} + \frac{i(4\pi\alpha_s)^2}{2\beta_2^+ \beta_3^+ \mu_1^2 \mu_2^2} e^{-\mu_1 \Delta z} + \frac{-i(4\pi\alpha_s)^2}{4\beta_2^+ \beta_3^+ \mu_1 \mu_2^2 (\mu_1 + \mu_2)} e^{-(\mu_1 + \mu_2) \Delta z} \quad (\text{A126})$$

Applying the average over the impact parameter.

$$I_3 = -i \sum \text{Res} \quad (\text{A127})$$

$$= \frac{-(4\pi\alpha_s)^2}{2\beta^{+2} \mu^2} \left( 1 - \frac{1}{2} e^{-\mu\Delta z} \right)^2 \quad (\text{A128})$$

$$\text{Tr} \langle \mathcal{M}_2 \mathcal{M}_0^* \rangle = \frac{N}{A_\perp} \frac{1}{d_A} C_2(R) C(R) (4\pi\alpha_s)^2 \int \rho(\Delta z) \int \frac{d^2 \mathbf{q}}{(2\pi)^2} P^{+2} |J(p)|^2 \frac{-1}{2\beta^{+2} \mu^4} \left( 1 - \frac{1}{2} e^{-\mu\Delta z} \right)^2 \quad (\text{A129})$$

*The momentum broadening distribution*

Recall the momentum broadening distribution,

$$\frac{dN^{(1)}}{d^3\vec{p}} = \text{Tr}\langle|\mathcal{M}_1|^2\rangle + 2\text{Re}\text{Tr}\langle|\mathcal{M}_2\mathcal{M}_0^*|\rangle \quad (\text{A130})$$

$$= \frac{N}{A_\perp} \frac{1}{d_A} C_2(R) C(R) (4\pi\alpha_s)^2 \int \rho(\Delta z) \int \frac{d^2\mathbf{q}}{(2\pi)^2} P^{+2} \left( |J(p-\mathbf{q})|^2 \frac{1}{\beta^{+2}\mu^4} \left( 1 - \frac{1}{2} e^{-\mu\Delta z} \right)^2 + 2|J(p)|^2 \times \right. \quad (\text{A131})$$

$$\left. \frac{-1}{2\beta^{+2}\mu^4} \left( 1 - \frac{1}{2} e^{-\mu\Delta z} \right)^2 \right) \quad (\text{A132})$$

$$= \frac{N}{A_\perp} \frac{1}{d_A} C_2(R) C(R) (4\pi\alpha_s)^2 \int \rho(\Delta z) \int \frac{d^2\mathbf{q}}{(2\pi)^2} (|J(p-\mathbf{q})|^2 - |J(p)|^2) \frac{4}{(1+\gamma)^2} \frac{1}{2\mu^4} \left( 1 - \frac{1}{2} e^{-\mu\Delta z} \right)^2 \quad (\text{A133})$$

**Appendix B: Formal subtleties**

In this appendix, we present results addressing two formal subtleties that arise from the inclusion of sub-eikonal corrections.

**Amplitude corrections from  $2 \rightarrow 2$  scattering.**

In this appendix we reproduce the differential cross section for a generic  $2 \rightarrow 2$  scattering process in QCD. This result is standard and can be found in many quantum field theory textbooks. Here we provide a concise summary following the treatment in Peskin and Schroeder [51], with the aim of motivating the structure of the scattering amplitude that will later be used to justify the need for corrections beyond the eikonal approximation.

*Scalar  $2 \rightarrow 2$  scattering*

For a scalar  $2 \rightarrow 2$  process in the centre-of-mass (CM) frame, the differential cross section is

$$\left( \frac{d\sigma}{d\Omega} \right)_{\text{CM}} = \frac{|\mathcal{M}|^2}{64\pi^2 E_{\text{CM}}^2}, \quad (\text{B1})$$

where all four external particles have the same mass.

For two massless incoming particles with momenta  $p, p'$  scattering into  $k, k'$ , the squared matrix element (averaged over initial spins and summed over final spins) is

$$\frac{1}{4} \sum_{\text{spins}} |\mathcal{M}|^2 = 8e^4 q^4 [(p \cdot k')(p' \cdot k) + (p \cdot k)(p' \cdot k')]. \quad (\text{B2})$$

Rewriting the matrix element in terms of the usual Mandelstam variables  $s, t, u$  gives

$$\frac{1}{4} \sum_{\text{spins}} |\mathcal{M}|^2 = \frac{8e^4}{t^2} (s^2 + u^2). \quad (\text{B3})$$

*Generalisation to QCD*

In QCD this generalises to

$$\frac{1}{4} \sum_{\text{spins}} |\mathcal{M}|^2 = \frac{8e^4 Q_i^2}{t^2} (s^2 + u^2), \quad (\text{B4})$$

where  $Q_i$  is the electric charge of a quark of flavour  $i$ . The corresponding CM-frame differential cross section is

$$\frac{d\sigma}{d\cos\theta_{\text{CM}}} = \frac{1}{32\pi s} \left( \frac{1}{4} \sum_{\text{spins}} |\mathcal{M}|^2 \right) = \frac{\pi\alpha^2 Q_i^2}{s} \left[ \frac{s^2}{t^2} + \frac{(s+t)^2}{t^2} \right]. \quad (\text{B5})$$

Using

$$t = -\frac{s}{2} (1 - \cos\theta_{\text{CM}}), \quad (\text{B6})$$

one finds

$$\frac{d\sigma}{dt} = \frac{2\pi\alpha^2 Q_i^2}{s^2} \left[ \frac{s^2}{t^2} + \frac{(s+t)^2}{t^2} \right]. \quad (\text{B7})$$

The important feature for our purposes is the scaling

$$\frac{d\sigma}{dt} \propto \frac{1}{s^2}. \quad (\text{B8})$$

#### *Implications for the eikonal amplitude*

For the diagram in fig. 1, the relevant kinematics give

$$s = (P^+ + \mathbf{q})^2, \quad s^2 = (P^+ + \mathbf{q})^4. \quad (\text{B9})$$

The scattering amplitude is taken to have the form

$$\frac{1}{2(2\pi)^3} |J(p)|^2 = f(p) \delta^{(2)}(p_\perp), \quad (\text{B10})$$

where  $f(p)$  contains the momentum dependence of the interaction. Using the result above,

$$f(p) = \frac{1}{s^2} = \frac{1}{(P^+ + \mathbf{q})^4}. \quad (\text{B11})$$

In the eikonal approximation, one assumes that the amplitude varies slowly with the transverse momentum transfer  $\mathbf{q}$ . This leads to the replacement  $J(p + \mathbf{q}) \approx J(p)$ , which is justified when  $f(p) \approx \frac{1}{P^{+4}}$ , since the large power-law suppression makes the energy dependence effectively insensitive to small  $\mathbf{q}$ .

However, in the present work we include sub-eikonal corrections, for which this simplification hold up to order  $1/P^{+4}$ . Once corrections of order  $1/P^{+4}$  are retained, the dependence on transverse momentum cannot be neglected, and one must keep the full structure  $J(p + \mathbf{q})$  rather than the purely eikonal approximation  $J(p) \propto \delta^{(2)}(p_\perp)$ . Thus, incorporating sub-eikonal effects requires improving the scattering amplitude beyond its leading-order, sharply localised form.

#### **The crossed diagram.**

One subtlety is that of the crossed diagram. The matrix is given by

$$\mathcal{M}_2^\times = ie^{ipx_0} \int \frac{d^2\mathbf{q}_{1,\perp}}{(2\pi)^2} \frac{dq_{1,z}}{2\pi} e^{-i\mathbf{q}_{1,\perp} \cdot \mathbf{b}_\perp} \frac{d^2\mathbf{q}_{2,\perp}}{(2\pi)^2} e^{-i\mathbf{q}_{2,\perp} \cdot \mathbf{b}_\perp} \frac{dq_{2,z}}{2\pi} J(p - q_1 - q_2) \times \quad (\text{B12})$$

$$\frac{1}{(p - q_1)^2 + i\epsilon} \frac{1}{(p - q_1 - q_2)^2 + i\epsilon} (2E)^2 v(\vec{\mathbf{q}}_1) v(\vec{\mathbf{q}}_2) e^{-iq_{1,z}(z_2 - z_0)} e^{-iq_{2,z}(z_1 - z_0)} \quad (\text{B13})$$

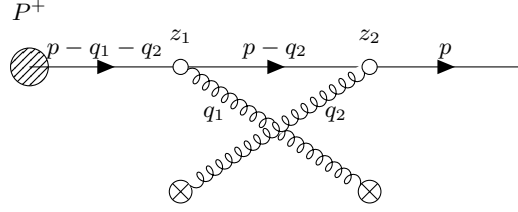


FIG. 5: Double scattering diagram with crossed gluon exchanges.

where one notes the change in the exponential factor

$$-i[q_{1,z}(z_2 - z_0) + q_{2,z}(z_1 - z_0)] = -i[q_{1,z}(z_2 - z_0) + q_{2,z}(z_1 - z_2 + z_2 - z_0)] \quad (B14)$$

$$= -i[(q_{1,z} + q_{2,z})(z_2 - z_0) + q_{2,z}(z_1 - z_2)] \quad (B15)$$

Calculating the first integral, one has

$$I_2^\times = \frac{-i(4\pi\alpha_s)}{\sqrt{2}P^+(q_{1,z} - i\mu_2)(q_{1,z} + i\mu_2)} \quad (B16)$$

which is the same result as the original GLV calculation but with  $1 \leftrightarrow 2$ .

In the case of  $I_3^\times$  one has  $z_2 - z_1 < 0$  where previously one had  $z_2 - z_1 > 0$ . We will therefore close the contour in the upper half of the complex plane and use the poles in the upper half of the complex plane.

The three poles in the upper half of the complex plane are

$$q_{1,z}^{(1)} = i\mu_1 \quad (B17)$$

$$q_{1,z}^{(2)} = i\mu_2 \quad (B18)$$

$$q_{1,z}^{(3)} = \sqrt{2}P^+ \quad (B19)$$

Resulting in

$$I_3^\times = \frac{-i4\pi\alpha_s}{\sqrt{2}P^+} \left( \frac{1}{2\mu_1^2\mu_2^2} + \frac{1}{(\sqrt{2}P^+)^4} \right) \quad (B20)$$

Consequently, the contribution from the crossed diagram appears at order  $\frac{1}{P^{+4}}$ . More importantly, this correction implies that the double scattering result is no longer equal to the single scattering result, signaling a violation of unitarity if one were to include this diagram.

## VIII. ACKNOWLEDGMENTS

We thank Ofentse Matlhkola, Cole Faraday, Will Horowitz and Fabio Dominguez for productive discussions and their valuable insights. DVDB and IK thank the National Research Foundation, the National Institute for Theoretical and Computational Sciences (NITheCS), and the SA-CERN collaboration for their generous financial support during the course of this work. This work is supported by the DST/NRF in South Africa under Thuthuka grant number TTK240313208902.

## IX. REFERENCES

[1] S. Acharya *et al.* (ALICE), *Eur. Phys. J. C* **84**, 813 (2024), arXiv:2211.04384 [nucl-ex].

[2] U. Heinz and R. Snellings, *Ann. Rev. Nucl. Part. Sci.* **63**, 123 (2013), arXiv:1301.2826 [nucl-th].

[3] W. Busza, K. Rajagopal, and W. van der Schee, *Ann. Rev. Nucl. Part. Sci.* **68**, 339 (2018), arXiv:1802.04801 [hep-ph].

[4] A. Majumder and M. Van Leeuwen, *Prog. Part. Nucl. Phys.* **66**, 41 (2011), arXiv:1002.2206 [hep-ph].

[5] G.-Y. Qin and X.-N. Wang, *Int. J. Mod. Phys. E* **24**, 1530014 (2015), arXiv:1511.00790 [hep-ph].

[6] J. Adam *et al.* (ALICE), *JHEP* **09**, 170, arXiv:1506.03984 [nucl-ex].

[7] G. Aad *et al.* (ATLAS), *Phys. Rev. Lett.* **131**, 072301 (2023), arXiv:2206.01138 [nucl-ex].

[8] S. Chatrchyan *et al.* (CMS), *Phys. Rev. C* **84**, 024906 (2011), arXiv:1102.1957 [nucl-ex].

[9] M. Spousta, *Mod. Phys. Lett. A* **28**, 1330017 (2013), arXiv:1305.6400 [hep-ex].

[10] L. Adamczyk *et al.* (STAR), *Phys. Rev. C* **96**, 024905 (2017), arXiv:1702.01108 [nucl-ex].

[11] S. Acharya *et al.* (ALICE), *Phys. Lett. B* **864**, 139409 (2025), arXiv:2411.03106 [nucl-ex].

[12] G. Aad *et al.* (ATLAS), *Phys. Lett. B* **871**, 139929 (2025), arXiv:2504.04805 [nucl-ex].

[13] V. Chekhovskiy *et al.* (CMS), *JHEP* **06**, 120, arXiv:2502.13020 [nucl-ex].

[14] B. E. Aboona *et al.* (STAR), *Phys. Rev. Lett.* **134**, 232301 (2025), arXiv:2309.00156 [nucl-ex].

[15] R. Baier, Y. L. Dokshitzer, A. H. Mueller, S. Peigne, and D. Schiff, *Nucl. Phys. B* **483**, 291 (1997), arXiv:hep-ph/9607355.

[16] J. Casalderrey-Solana and D. Teaney, *JHEP* **04**, 039, arXiv:hep-th/0701123.

[17] X.-N. Wang and U. A. Wiedemann (2025) arXiv:2508.18794 [hep-ph].

[18] M. Gyulassy, P. Levai, and I. Vitev, *Nucl. Phys. A* **661**, 637 (1999), arXiv:hep-ph/9907343.

[19] M. Gyulassy, P. Levai, and I. Vitev, in *1999 International Europhysics Conference on High-Energy Physics* (1999) pp. 971–973.

[20] M. Gyulassy, P. Levai, and I. Vitev, *Nucl. Phys. B* **571**, 197 (2000), arXiv:hep-ph/9907461.

[21] M. Gyulassy, P. Levai, and I. Vitev, *Phys. Rev. Lett.* **85**, 5535 (2000), arXiv:nucl-th/0005032.

[22] M. Gyulassy, P. Levai, and I. Vitev, *Nucl. Phys. B* **594**, 371 (2001), arXiv:nucl-th/0006010.

[23] I. Vitev, M. Gyulassy, and P. Levai, *Acta Phys. Hung. A* **17**, 237 (2003), arXiv:nucl-th/0204019.

[24] R. Baier, Y. L. Dokshitzer, S. Peigne, and D. Schiff, *Phys. Lett. B* **345**, 277 (1995), arXiv:hep-ph/9411409.

[25] R. Baier, Y. L. Dokshitzer, A. H. Mueller, S. Peigne, and D. Schiff, *Nucl. Phys. B* **484**, 265 (1997), arXiv:hep-ph/9608322.

[26] R. Baier, Y. L. Dokshitzer, A. H. Mueller, and D. Schiff, *Nucl. Phys. B* **531**, 403 (1998), arXiv:hep-ph/9804212.

[27] N. Armesto, C. A. Salgado, and U. A. Wiedemann, *Phys. Rev. D* **69**, 114003 (2004), arXiv:hep-ph/0312106.

[28] M. Connors, C. Nattrass, R. Reed, and S. Salur, *Rev. Mod. Phys.* **90**, 025005 (2018), arXiv:1705.01974 [nucl-ex].

[29] Y. Mehtar-Tani, J. G. Milhano, and K. Tywoniuk, *Int. J. Mod. Phys. A* **28**, 1340013 (2013), arXiv:1302.2579 [hep-ph].

[30] S. Cao and X.-N. Wang, *Rept. Prog. Phys.* **84**, 024301 (2021), arXiv:2002.04028 [hep-ph].

[31] G.-Y. Qin, J. Ruppert, C. Gale, S. Jeon, G. D. Moore, and M. G. Mustafa, *Phys. Rev. Lett.* **100**, 072301 (2008), arXiv:0710.0605 [hep-ph].

[32] N.-B. Chang, Y. Tachibana, and G.-Y. Qin, *Phys. Lett. B* **801**, 135181 (2020), arXiv:1906.09562 [nucl-th].

[33] J. L. Nagle and W. A. Zajc, *Ann. Rev. Nucl. Part. Sci.* **68**, 211 (2018), arXiv:1801.03477 [nucl-ex].

[34] S. Acharya *et al.* (ALICE), *JHEP* **09**, 204, arXiv:2405.14511 [hep-ex].

[35] J. Adam *et al.* (ALICE), *JHEP* **11**, 127, arXiv:1506.08808 [nucl-ex].

[36] J. Brewer, A. Mazeliauskas, and W. van der Schee, in *Opportunities of OO and pO collisions at the LHC* (2021) arXiv:2103.01939 [hep-ph].

[37] J. Casalderrey-Solana, D. Gulhan, G. Milhano, D. Pablos, and K. Rajagopal, *JHEP* **03**, 135, arXiv:1609.05842 [hep-ph].

[38] G. Nijs and W. van der Schee, *Phys. Rev. C* **106**, 044903 (2022), arXiv:2110.13153 [nucl-th].

[39] G. Nijs, W. van der Schee, U. Gürsøy, and R. Snellings, *Phys. Rev. C* **103**, 054909 (2021), arXiv:2010.15134 [nucl-th].

[40] C. Beattie, G. Nijs, M. Sas, and W. van der Schee, *Phys. Lett. B* **836**, 137596 (2023), arXiv:2203.13265 [nucl-th].

[41] W. van der Schee, I. Kolbé, G. Nijs, K. Ruhani, I. Ahmed, and S. Iqbal, arXiv (2025), arXiv:2509.04299 [nucl-th].

[42] C. Faraday and W. A. Horowitz, *JHEP* **11**, 019, arXiv:2505.14568 [hep-ph].

[43] C. Faraday and W. A. Horowitz, *Phys. Lett. B* **864**, 139437 (2025), arXiv:2411.09647 [hep-ph].

[44] D. Pablos and A. Takacs, arXiv (2025), arXiv:2509.19430 [hep-ph].

[45] M. Gyulassy, P. Levai, and I. Vitev, *Phys. Rev. D* **66**, 014005 (2002), arXiv:nucl-th/0201078.

[46] J.-w. Qiu and I. Vitev, *Phys. Lett. B* **570**, 161 (2003), arXiv:nucl-th/0306039.

[47] A. V. Sadofyev, M. D. Sievert, and I. Vitev, *Phys. Rev. D* **104**, 094044 (2021), arXiv:2104.09513 [hep-ph].

[48] I. Kolbe and W. A. Horowitz, *Phys. Rev. C* **100**, 024913 (2019), arXiv:1511.09313 [hep-ph].

[49] I. Kolbe, *Short path length pQCD corrections to energy loss in the quark gluon plasma*, Master’s thesis, Cape Town U. (2015), arXiv:1509.06122 [hep-ph].

[50] M. Li, T. Lappi, X. Zhao, and C. A. Salgado, *Phys. Rev. D* **108**, 036016 (2023), arXiv:2305.12490 [hep-ph].

[51] M. E. Peskin and D. V. Schroeder, *An Introduction to quantum field theory* (Addison-Wesley, Reading, USA, 1995).